

---

# DECOUPLING TIME AND RISK: RISK-SENSITIVE REINFORCEMENT LEARNING WITH GENERAL DISCOUNTING

---

**Mehrdad Moghimi**

Dept. of Mathematics and Statistics  
York University  
Toronto, Canada  
moghimi@yorku.ca

**Anthony Coache**

Dept. of Mathematics  
Imperial College London  
London, United Kingdom  
a.coache@imperial.ac.uk

**Hyejin Ku**

Dept. Mathematics and Statistics  
York University  
Toronto, Canada  
hku@yorku.ca

## ABSTRACT

Distributional reinforcement learning (RL) is a powerful framework increasingly adopted in safety-critical domains for its ability to optimize risk-sensitive objectives. However, the role of the discount factor is often overlooked, as it is typically treated as a fixed parameter of the Markov decision process or tunable hyperparameter, with little consideration of its effect on the learned policy. In the literature, it is well-known that the discounting function plays a major role in characterizing time preferences of an agent, which an exponential discount factor cannot fully capture. Building on this insight, we propose a novel framework that supports flexible discounting of future rewards and optimization of risk measures in distributional RL. We provide a technical analysis of the optimality of our algorithms, show that our multi-horizon extension fixes issues raised with existing methodologies, and validate the robustness of our methods through extensive experiments. Our results highlight that discounting is a cornerstone in decision-making problems for capturing more expressive temporal and risk preferences profiles, with potential implications for real-world safety-critical applications.

**Keywords** Reinforcement Learning · Discount Function · Distributional Reinforcement Learning · Risk-Sensitivity · Stock-augmentation

## 1 Introduction

In the standard formulation of reinforcement learning (RL) problems, a key component is the discount factor, denoted by  $\gamma$ , which applies exponential discounting to future rewards. Discounting encodes time preferences of the agent, models unknown termination times, and generally reduces approximation errors and variance from distant rewards [Petrik & Scherrer, 2008, Amit et al., 2020], altogether leading to more stable learning algorithms. While mathematically convenient, this paradigm may create fundamental challenges in more complex settings. Choosing  $\gamma \in (0, 1)$  can render the agent's actions ineffective at altering return distributions over long timescales [see e.g., Pires et al., 2025]. On the other hand, choosing  $\gamma$  close to one to extend the agent's effective horizon can be impractical, since the variance of temporal-difference updates grows sharply as  $\gamma \rightarrow 1$ , leading to severe training instability and slow convergence [Naik et al., 2019].

Most importantly, exponential discounting *cannot* capture some preference reversals that characterize humans' and animals' behaviors for various long-horizon planning tasks. Let us revisit this hypothetical scenario from Fedus et al. [2019]: suppose that someone offers to a risk-neutral agent, without any risk, either \$1 at time  $t$  or \$1.1 at time  $t + 1$ . Under exponential discounting, the agent would prefer the same reward for any time  $t$ . In contrast, for some parametrizations of hyperbolic discounting, the agent would select \$1 if  $t = 0$  but \$1.1 if  $t = 365$ . This remains true for a risk-sensitive agent, as long as the reward distributions yield risk measures of the same monetary values.

Green & Myerson [2004] explained that preference inconsistencies, such as impulsivity or self-control, arise when choice options differ on many dimensions: (i) magnitude of the rewards, inherently embedded in the reward function; (ii) time elapsed before receiving the rewards; and (iii) likelihood of receiving the rewards. While some special cases of preference modeling admit consistent preferences across such dimensions, i.e., reward scaling for risk-neutral agents with an exponential discount factor, this is generally not the case and modeling time preferences through a single scalar discount factor can be overly restrictive. Therefore, to accurately describe time and risk preferences of an arbitrary

agent, an RL algorithm should allow different characterizations of the discounting (second dimension) and objective function (third dimension), resulting in a wider range of preference profiles and optimal strategies.

Despite their central role in behavioral decision research, these dimensions have not been systematically integrated into RL models. On one hand, several works have considered general discounting schemes, including state-dependent [White, 2017, Pitis, 2019] and adaptive discount factors [François-Lavet et al., 2016, Xu et al., 2018, Zahavy et al., 2020]. On the other hand, a large body of research aimed to move beyond expectation-based goal functionals, leading to a plethora of risk-sensitive RL algorithms [Bäuerle & Ott, 2011, Tamar et al., 2017, Di Castro et al., 2019] including distributional RL [Morimura et al., 2010, Bellemare et al., 2017]. While these two lines of work address complementary aspects of preference modeling, they have largely been developed in isolation. We provide more discussion on related works in Appendix A.

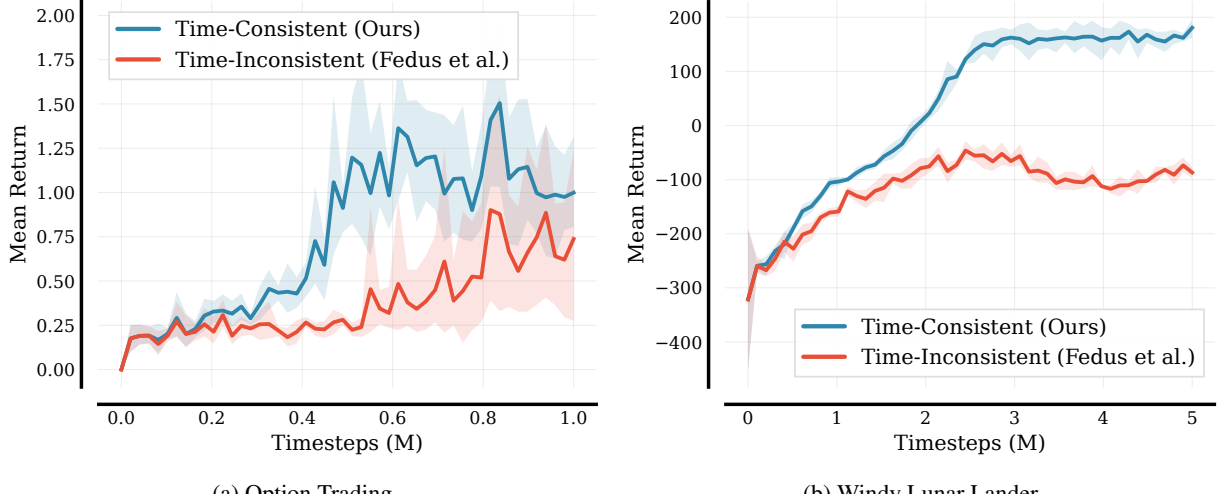


Figure 1: **The impact of Time-Consistency.** Performance comparison between our proposed time-consistent framework (in blue) and the time-inconsistent approach of Fedus et al. [2019] (in red). By correctly modeling the non-stationary optimal policy required for general discounting, our method achieves higher returns in American Put Option Trading (Fig. 1a) and Windy Lunar Lander (Fig. 1b).

A notable work by Fedus et al. [2019] attempted to introduce hyperbolic discounting into deep RL, but overlooked the fundamental need for time-dependent policies, as noted by Schultheis et al. [2022]. By enforcing stationarity on a problem where the optimal strategy is inherently non-stationary, their approach violates time consistency, which requires that a policy determined to be optimal at the initial time remains optimal at all future decision points. Figure 1 illustrates this critical distinction: our time-consistent approach, which properly accounts for non-stationarity, significantly outperforms the time-inconsistent baseline in both financial and control tasks. We further demonstrate in our experiments that these performance gains scale beyond simple environments by validating our methodology on high-dimensional Atari games.

This exposes a critical gap: how can we enable general discount functions *and* risk-sensitive reasoning without incurring instability or abandoning the intuitive framework of optimizing a utility over total return? In this work, we answer by extending the theory of stock-augmented distributional RL to allow general discounting approaches *and* a richer class of objective functions. Our contributions are summarized as follows:

- We provide a unified framework for stock augmentation in distributional RL with general discount functions and optimized certainty equivalent (OCE) risk measures, which builds upon the stock-augmented return distribution optimization from Pires et al. [2025].
- We devise RL algorithms for the finite-horizon, multi-horizon and infinite-horizon cases, and establish performance bounds for the approximation error between the algorithm’s policies and optimal policy.
- We demonstrate the performance of our algorithms on various benchmark environments. We use a goal-based wealth management problem to investigate the effects of both the discounting and objective function in shaping the agent’s preference profiles, and Atari games to show improvements when using multi-horizon learning for complex high-dimensional environments.

Incorporating stock into distributional dynamic programming (DP) as in the framework of Pires et al. [2025], where the agent’s state is augmented with a statistic that tracks the history of accumulated rewards, allows the optimization of

risk-sensitive statistical functionals that would not be possible otherwise. In fact, for finite-horizon problems, we show that including general discounting and OCE risk measures may be done seamlessly within the realm of stock-augmented distributional RL. We also describe how our approach may be adapted to the multi-timescale RL paradigm [see e.g., Masset et al., 2025]. In doing so, we fix the incoherence in the former approach of Fedus et al. [2019] regarding the time representation (see Section 4), and highlight how this significantly improves the performance. For infinite-horizon problems, we borrow ideas from Hau et al. [2023] to develop an algorithm where the agent follows a risk-sensitive policy with general discounting over a planning horizon, and approximates the problem beyond it with a risk-neutral policy with exponential discounting. The approach we use for the performance analysis of the resulting policy, however, is quite different from the original work, as it relies on stock augmentation and can be extended to Mean-CVaR risk measures.

In this paper, we first recall the RL framework from Pires et al. [2025] in Section 2. We then extend the setting to general discount functions and OCE risk measures for finite-horizon problems in Section 3, provide a multi-horizon approach for simultaneously learning over many discount factors in Section 4, and derive an approximate algorithm with convergence guarantees for infinite-horizon problems in Section 5. We conclude the paper with experiments and ablation studies to demonstrate the performance of our general discounting risk-sensitive distributional RL algorithms in Section 6.

## 2 Stock-Augmented Return Distribution Optimization

**Notation.** We use  $\Delta(\mathbb{R}^n)$  to denote the set of probability distribution functions over  $\mathbb{R}^n$ , and  $\text{df}(\cdot)$  denotes the distribution of a random variable. For a finite set of  $n \in \mathbb{N}$  outcomes,  $\Delta(n)$  denotes the corresponding  $|n|$ -dimensional probability simplex. We denote the (resp. supremum) 1-Wasserstein distance between distributions  $\nu, \nu' \in \Delta(\mathbb{R}^n)$  by  $w(\nu, \nu')$  (resp.  $\bar{w}(\nu, \nu')$ ).

The standard RL problem is typically modeled as a Markov decision process (MDP), defined by a tuple  $(\mathcal{S}, \mathcal{A}, P, R, \gamma)$ . Here,  $\mathcal{S}$  is the state space,  $\mathcal{A}$  is the action space,  $P : \mathcal{S} \times \mathcal{A} \rightarrow \Delta(\mathcal{S})$  is the transition function,  $R : \mathcal{S} \times \mathcal{A} \rightarrow \Delta(\mathbb{R})$  is the reward distribution, and  $\gamma \in (0, 1]$  is the discount factor. The agent’s goal is to find a policy  $\pi : \mathcal{S} \rightarrow \Delta(\mathcal{A})$  that maximizes the expected value of the discounted return,

$$G_t^\gamma \doteq \sum_{k=0}^{\infty} \gamma^k R_{t+k+1}. \quad (1)$$

Here, we use the superscript  $\gamma$  to emphasize the dependence on the discount factor and  $R_t$  is interpreted as a random variable resulting from the agent taking action  $A_t$  in state  $S_t$ , thus  $G^\gamma$  implicitly depends on the policy  $\pi$ .

Pires et al. [2025] generalize this problem to the optimization of arbitrary statistical functionals of a multivariate return distribution, a problem they term *return distribution optimization*. In their framework, the reward signal can be a vector-valued pseudo-reward  $R_t \in \mathcal{C} \doteq \mathbb{R}^m$ . To solve this broader class of problems using DP, they introduce *stock augmentation*, in which the environment’s state  $s \in \mathcal{S}$  is augmented with a *stock* vector  $c \in \mathcal{C}$ . The stock tracks a scaled history of accumulated rewards, and its recursive property is defined by the update rule  $C_{t+1}^\gamma \doteq \gamma^{-1} (C_t^\gamma + R_{t+1})$ , which originates from the expanded form  $C_t^\gamma = \gamma^{-t} (C_0^\gamma + \sum_{k=0}^{t-1} \gamma^k R_{k+1})$ . The agent’s policy  $\pi$  then becomes a function of the augmented state  $(s, c) \in \mathcal{S} \times \mathcal{C}$ .

The optimization objective is to find a policy  $\pi$  that maximizes a functional  $F_K$  applied to the distribution of the total outcome from the start of the episode, i.e., the initial stock plus the total discounted return,  $C_0^\gamma + G_0^\gamma$ . The functional  $F_K$  is derived from a statistical functional  $K : \Delta(\mathcal{C}) \rightarrow \mathbb{R}$  that quantifies risk preferences over return distributions. For a given return distribution function  $\eta_\pi^\gamma : \mathcal{S} \times \mathcal{C} \rightarrow \Delta(\mathbb{R})$  defined by  $\eta_\pi^\gamma(s, c) \doteq \text{df}(G^\gamma(s, c))$ , the objective is defined as

$$(F_K \eta_\pi^\gamma)(s, c) \doteq K \text{df}(c + G(s, c)),$$

where  $G(s, c) \sim \eta_\pi^\gamma(s, c)$ . In particular, taking  $K$  as the expectation reduces to the standard risk-neutral RL problem. The return distribution optimization problem is thus to find  $\sup_\pi F_K \eta_\pi^\gamma$  evaluated at the initial state  $(s_0, c_0)$ .

A key challenge for DP is that decisions are made at time  $t > 0$ , but the objective is defined over the total outcome from time  $t = 0$ . Pires et al. [2025] resolve this by demonstrating a crucial relationship between the total outcome and the state of the system at time  $t$  (see Appendix C for derivation):

$$C_0^\gamma + G_0^\gamma \stackrel{\mathcal{D}}{=} \gamma^t (C_t^\gamma + G_t^\gamma). \quad (2)$$

This scaling relationship reveals that the quantity  $C_t^\gamma + G_t^\gamma$  serves as an “anytime proxy” for the original objective. To make this proxy useful for optimization, we introduce two key properties for an objective functional  $K$ .

**Definition 2.1** (Indifference to Scaling). For all distributions  $\nu, \nu' \in (\Delta(\mathcal{C}), \mathbf{w})$  such that  $K\nu \geq K\nu'$ , then  $K(\gamma G) \geq K(\gamma G')$ , where  $G \sim \nu$ ,  $G' \sim \nu'$  and  $K(G) = K\text{df}(G)$ .

**Definition 2.2** (Indifference to Mixtures). For every  $\eta, \eta' \in (\Delta(\mathcal{C})^{\mathcal{S} \times \mathcal{C}}, \bar{\mathbf{w}})$  such that  $K\eta(s, c) \geq K\eta'(s, c)$  for all  $(s, c) \in \mathcal{S} \times \mathcal{C}$ , then for any random variable  $(S, C)$  taking values in  $\mathcal{S} \times \mathcal{C}$  we also have  $K(G(S, C)) \geq K(G'(S, C))$ , where  $G(s, c) \sim \eta(s, c)$  and  $G'(s, c) \sim \eta'(s, c)$ .

The *indifference to scaling* ensures that preferences are preserved under scaling by  $\gamma$ . This allows a policy that improves the objective over the “anytime proxy” to also improve the original objective over  $C_0^\gamma + G_0^\gamma$ . The *indifference to mixtures* property states that if a set of outcome distributions is preferred to another on a component-wise basis, then any probabilistic mixture of the former is also preferred to the same mixture of the latter. This guarantees the monotonicity of the Bellman operator.

With these theoretical underpinnings, Pires et al. [2025] develop *distributional DP* methods. These methods rely on the *stock-augmented distributional Bellman operator* for a stationary policy  $\pi$  and return distribution function  $\eta$ :

$$(\mathcal{T}_\pi^\gamma \eta)(s, c) \doteq \text{df}(R_{t+1} + \gamma G(S_{t+1}, C_{t+1}^\gamma)), \quad (3)$$

where  $(S_t, C_t) = (s, c)$ ,  $(S_{t+1}, R_{t+1}) \sim P(\cdot | s, A_t)$ ,  $A_t \sim \pi(s, c)$ , and  $G \sim \eta(S_{t+1}, (c + R_{t+1})/\gamma)$ . The true return distribution function for a policy  $\pi$ , denoted  $\eta_\pi^\gamma$ , is the unique fixed point of this operator satisfying the distributional Bellman equation:  $\eta_\pi^\gamma = \mathcal{T}_\pi^\gamma \eta_\pi^\gamma$ .

Moving from policy evaluation to control requires selecting actions that greedily improve the objective functional  $F_K$ . A greedy policy  $\bar{\pi}$  with respect to any distribution function  $\eta$  is one that satisfies  $F_K \mathcal{T}_{\bar{\pi}}^\gamma \eta = \sup_{\pi' \in \Pi} F_K \mathcal{T}_{\pi'}^\gamma \eta$ . This is implemented by selecting the action  $a^*$  at state  $(s, c)$  that maximizes the objective over the possible one-step outcomes:

$$a^*(s, c) \in \arg \max_{a \in \mathcal{A}} (F_K(\mathcal{T}_{\pi_a}^\gamma \eta))(s, c),$$

where  $\pi_a$  is the policy that deterministically selects action  $a \in \mathcal{A}$ . For the important special case of expected utilities, where  $F_K = U_f$  for some function  $f : \mathcal{C} \rightarrow \mathbb{R}$ , the optimal greedy policy selects the action that maximizes the expected utility of the immediate outcome:

$$a^*(s, c) \in \arg \max_{a \in \mathcal{A}} \mathbb{E} f(c + G(s, c, a)),$$

where  $G(s, c, a)$  is a random variable drawn from the distribution  $(\mathcal{T}_{\pi_a}^\gamma \eta)(s, c)$ . These operators form the basis of distributional value and policy iteration algorithms that can find optimal policies with respect to the functional  $F_K$ .

### 3 General Discounting in Finite Horizon

We extend the stock-augmented distributional RL framework to settings with general time preferences. Let  $d : \mathbb{N}_0 \rightarrow \mathbb{R}^+$  be a general discount function, and define the *one-step discount factor* as  $\hat{d}_t \doteq d_{t+1}/d_t$  where  $d_t \doteq d(t)$ . We make an intuitive assumption that  $d_0 = 1$  and  $d_t$  is non-increasing, i.e.,  $d_{t+1} \leq d_t$  for all  $t \geq 0$ . This aligns with the economic principle that future rewards are not valued more than present ones and is general enough to include exponential, hyperbolic, and quasi-hyperbolic discounting models. The non-increasing property implies that  $\hat{d}_t \in (0, 1]$  for all  $t$ .

The discounted return from time step  $t$  over a finite horizon  $T \in \mathbb{N}$  is given by  $G_t^d \doteq \frac{1}{d_t} \sum_{k=t}^{T-1} d_k R_{k+1}$ . We also define the stock  $C_t^d = \frac{1}{d_t} \left( C_0^d + \sum_{k=0}^{t-1} d_k R_{k+1} \right)$ , which evolves according to a general discount function with an update rule of  $C_{t+1}^d = (C_t^d + R_{t+1}) / \hat{d}_t$ . If we set  $d_t = \gamma^t$ , we recover the exponentially discounted stock from Pires et al. [2025]. The key benefit of the stock is that it helps finding the “anytime proxy” for the total outcome, in a similar manner to (2). The total unscaled return from time zero, which is the object of a static utility function, may be expressed recursively using the current stock  $C_t^d$  and the future return  $G_t^d$  (see Appendix C for derivation):

$$C_0^d + G_0^d \stackrel{D}{=} d_t (C_t^d + G_t^d). \quad (4)$$

This recursive structure allows us to define a DP operator. However, the non-stationarity of  $\hat{d}_t$  implies the operator and optimal policy are time-dependent. Therefore, in this section, we assume a finite and known problem horizon  $T$ , which ensures the problem is well-posed and enables an exact solution via backward induction. This assumption is necessary because for general discount functions, such as hyperbolic,  $\hat{d}_t \rightarrow 1$  as  $t \rightarrow \infty$ . This violates the contraction mapping condition required for standard infinite-horizon DP, rendering the problem potentially ill-posed. We address the infinite-horizon case and its implications in Section 5.

A non-stationary policy is a sequence  $\pi = (\pi_0, \dots, \pi_{T-1})$ , where  $\pi_t : \mathcal{S} \times \mathcal{C} \rightarrow \Delta(\mathcal{A})$ . For a return distribution function  $\eta_t^\pi(s, c) \doteq \text{df}(G_t^d(s, c))$ , similarly to equation (3), we define the *time-dependent distributional Bellman operator* for a policy  $\pi_t$  at time  $t$  and a next-step distribution function  $\eta_{t+1}$  as

$$(\mathcal{T}_{\pi_t}^d \eta_{t+1})(s, c) \doteq \text{df} \left( R_{t+1} + \hat{d}_t G_{t+1}^d(S_{t+1}, C_{t+1}^d) \right),$$

where the distribution is over  $S_{t+1} \sim P(\cdot|s, A_t)$  and  $R_{t+1} \sim R(\cdot|s, A_t)$ , with  $A_t \sim \pi_t(\cdot|s, c)$ , and  $G_{t+1}^d \sim \eta_{t+1}^\pi(S_{t+1}, (c + R_{t+1})/\hat{d}_t)$ . In this framework, an agent can use the learned distribution  $\eta^\pi$  to reconstruct the distribution of the total outcome via (4) and select actions to optimize a static functional of that outcome. This requires establishing new theoretical guarantees for stock and time-augmented distributional DP.

The adoption of non-stationary return distributions allows us to relax the indifference to scaling assumption in Definition 2.1. We achieve this by directly optimizing the initial return distribution via the following objective:

$$(F_K \eta_t^\pi)(s, c) \doteq K \text{df}(d_t c + d_t G(s, c)) / d_t.$$

Notably, in the special case where the objective functional satisfies indifference to scaling (i.e., Definition 2.1), this formulation naturally recovers the objective proposed by Pires et al. [2025] for exponential discounting. This flexibility allows our stock-augmented framework to accommodate optimized certainty equivalent (OCE) risk measures, a broad class of convex risk measures originally developed for financial risk management [Ben-Tal & Teboulle, 2007]. For a random variable  $G$ , the OCE with respect to a utility function  $f : \mathbb{R} \rightarrow [-\infty, \infty)$  is defined as:

$$\text{OCE}_f(G) \doteq \max_{c_0 \in \mathcal{C}} \{-c_0 + \mathbb{E}[f(c_0 + G)]\}. \quad (5)$$

Optimizing this metric decomposes into finding the optimal return distribution for any initial stock and then selecting the best  $c_0$ . Our distributional DP framework solves the former simultaneously for all  $c \in \mathcal{C}$  by setting the objective functional to  $(U_f \eta_t)(s, c) \doteq \mathbb{E}[f(d_t c + d_t G_t)] / d_t$ . Consequently, the OCE value is obtained by maximizing the scalar function  $J(c_0) \doteq -c_0 + (U_f \eta_0^*)(s_0, c_0)$  over the learned value surface. As in Pires et al. [2025], we perform this outer optimization via grid search over a discretized set  $\bar{\mathcal{C}} \subset \mathcal{C}$ . Figure 2 illustrates the utility functions  $f$  associated with several common risk measures. While some instances, such as Mean-CVaR, satisfy the indifference to scaling property, others, such as Entropic Risk and Mean-Variance, do not.

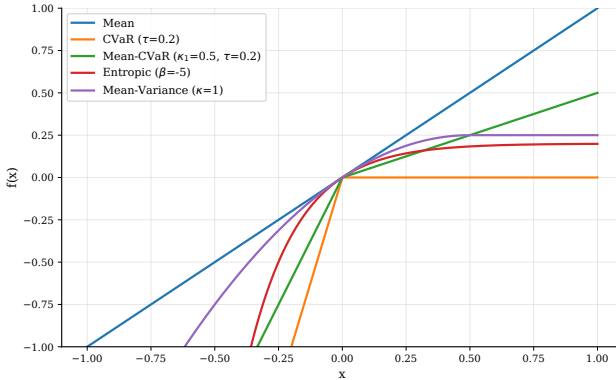


Figure 2: **Utility functions for common OCE risk measures.** Detailed formulations are provided in Appendix D.

In the finite-horizon setting, the optimal policy can be determined via backward induction. The theoretical validity of this procedure relies on the following Time-Dependent Monotonicity Lemma. The proof is deferred to Appendix E.1.

**Lemma 3.1** (Time-Dependent Monotonicity). *Let  $K$  be an objective functional satisfying the indifference to mixture property. For any time  $t < T$ , let  $\eta_{t+1}$  and  $\eta'_{t+1}$  be two return distribution functions for time  $t+1$ . If  $F_K \eta_{t+1} \geq F_K \eta'_{t+1}$ , then for any time- $t$  policy  $\pi_t$ :  $F_K(\mathcal{T}_{\pi_t}^d \eta_{t+1}) \geq F_K(\mathcal{T}_{\pi_t}^d \eta'_{t+1})$ .*

Equipped with this lemma, we formally establish the optimality of our approach. We refer to Appendix E.2 for the proof.

**Theorem 3.2** (Optimality of Distributional Backward Induction). *Let the problem horizon  $T \in \mathbb{N}$  be finite and known, and let the objective functional  $K$  be indifferent to mixtures. Assume that the sequence of return distributions  $\eta^* = (\eta_0^*, \dots, \eta_T^*)$  is generated by the following backward induction algorithm:*

- **Base Case:** For all  $(s, c) \in \mathcal{S} \times \mathcal{C}$ , set  $\eta_T^*(s, c) = \delta_0$ .

- **Recursive Step:** For  $t = T - 1$  down to 0, compute  $\eta_t^* \doteq \mathcal{T}_*^d \eta_{t+1}^*$ , where  $\mathcal{T}_*^d$  is the greedy time-dependent distributional Bellman operator, defined such that for any function  $\eta_{t+1}$  and for all  $(s, c) \in \mathcal{S} \times \mathcal{C}$ , it returns the function  $\eta_t$  satisfying:

$$(F_K \eta_t)(s, c) = \sup_{\pi_t} (F_K(\mathcal{T}_{\pi_t}^d \eta_{t+1}))(s, c).$$

Then, the sequence  $\eta^*$  is a sequence of optimal return distributions. Furthermore, the non-stationary policy  $\pi^* = (\pi_0^*, \dots, \pi_{T-1}^*)$ , where each  $\pi_t^*$  is a greedy policy with respect to  $\eta_{t+1}^*$ , is optimal for any initial augmented state.

**Remark 3.3** (On Tie-Breaking and Uniqueness). The greedy operator  $\mathcal{T}_*^d$  may not be unique, as multiple actions (or stochastic mixtures) can yield distributions that are optimal with respect to  $F_K$  [see e.g. Section 7.5 of Bellemare et al., 2023]. Consequently, the optimal policy  $\pi^*$  may not be unique. A greedy policy  $\pi_t^*$  is any policy that, at each state  $(s, c)$ , selects a distribution over actions that achieves the supremum. All such greedy policies are optimal.

**Remark 3.4** (On Lipschitz Continuity). The optimality guarantee for the exact inner problem (Theorem 3.2) relies solely on monotonicity and does not require the objective functional  $K$  to be Lipschitz continuous. This contrasts with the infinite-horizon setting of Pires et al. [2025], where Lipschitz continuity is essential for convergence. However, for the full OCE problem, the Lipschitz property is strictly necessary: it ensures the outer optimization over  $c_0$  is well-conditioned (bounding discretization error) and controls error propagation in the approximate DP.

While not required for exact planning, Lipschitz continuity becomes essential for analyzing the error in any practical algorithm that must approximate the return distribution. Proposition 3.5 provides a bound for the total suboptimality of the approximate algorithm, accounting for both inner approximation and outer discretization errors (see proof in Appendix E.3).

**Proposition 3.5** (OCE Optimality Bound). *Let  $f : \mathbb{R} \rightarrow \mathbb{R}$  be an  $L$ -Lipschitz utility function. Let  $\pi^*$  be the optimal policy from Theorem 3.2, and let  $\hat{\pi}$  be the policy derived from an approximate backward induction with one-step errors  $(\varepsilon_0, \dots, \varepsilon_{T-1})$ . Let the outer optimization be performed over a finite grid  $\bar{\mathcal{C}}$  with spacing  $\delta$ . If  $\hat{c} \in \bar{\mathcal{C}}$  denotes the initial stock selected by the algorithm, and  $\mathcal{E}_{DP} \doteq L \sum_{t=0}^{T-1} d_t \varepsilon_t$  denotes the cumulative DP error term, the total suboptimality is bounded by*

$$\text{OCE}_f(\eta_0^*) - (-\hat{c} + \mathbb{E}[f(\hat{c} + G^{\hat{\pi}})]) \leq 2\mathcal{E}_{DP} + \frac{(1+L)\delta}{2}.$$

## 4 Multi-Horizon Approximation for General Discounting

Many discount functions, such as hyperbolic, can be expressed as a weighted integral of exponential discount functions,

$$d_t = \int_0^1 \gamma^t w(\gamma) d\gamma, \quad (6)$$

where  $w : [0, 1] \rightarrow \mathbb{R}$  is a weighting function over the discount factor  $\gamma$ . This integral can be approximated with a discrete Riemann sum over a fixed set of  $m$  exponential discount factors  $\Gamma = \{\gamma_1, \dots, \gamma_m\}$  as  $d_t \approx \tilde{d}_t \doteq \sum_{i=1}^m w_i \gamma_i^t$ , where the weights  $w_i = w(\gamma_i)(\gamma_i - \gamma_{i-1})$  are derived from the weighting function. Fedus et al. [2019] uses this fact to derive a stationary value function  $Q^d(s, a) = \int_0^1 Q^\gamma(s, a) w(\gamma) d\gamma$  under the general discount functions of the form (6).

While this technique can be practically effective, it is theoretically incoherent. The resulting stationary policy,  $\pi(s)$ , greedily optimizes a local objective that resets at every time step, and is therefore not guaranteed to be optimal for any single, fixed global objective. As Schultheis et al. [2022] note, this stationary policy is also structurally incapable of modeling the preference reversal in hyperbolic discounting. To correctly optimize a global objective with any general discount function  $d_t$ , the passage of time must be an explicit part of the state representation. As formalized by Schultheis et al. [2022] for continuous-time problems, the value function must be non-stationary, which in discrete time corresponds to a time-dependent Bellman optimality equation:

$$Q_t^d(s, a) = R(s, a) + \hat{d}_t \max_{a'} Q_{t+1}^d(s', a').$$

This formulation is theoretically coherent, as it finds the true optimal non-stationary policy that maximizes the single, fixed objective function defined at the start of the episode  $\mathbb{E}[\sum_{t=0}^T d_t R_t]$ . It provides a principled “top-down” solution for finding an optimal plan under the assumption of pre-commitment.

Compared to the backward induction algorithm in Section 3, the multi-horizon approach introduces an approximation error; however, simultaneously predicting returns over multiple time horizons serves as a strong auxiliary task that promotes richer state representations [Jaderberg et al., 2016]. Using the recursive structure of the stock-augmented distributional RL framework, we express the return in terms of  $m$  exponential discounts. From (1), the discounted

return for  $\gamma_i$  is  $G_t^{\gamma_i} = \sum_{k=0}^{T-t-1} \gamma_i^k R_{t+k+1}$ . The unscaled outcome under the approximate discount function  $\tilde{d}_t$  can then be written recursively, analogous to (4) (see Appendix C):

$$C_0^{\tilde{d}} + G_0^{\tilde{d}} \stackrel{\mathcal{D}}{=} \tilde{d}_t \left( C_t^{\tilde{d}} + \sum_{i=1}^m w_{i,t} G_t^{\gamma_i} \right), \quad (7)$$

where the time-dependent weights are  $w_{i,t} \doteq w_i \gamma_i^t / \tilde{d}_t$ . Because these weights vary with time, the resulting decision problem is non-stationary. Nevertheless, unlike general discount functions for which  $\hat{d}_t$  may approach 1, the multi-horizon approximation remains well-defined in the infinite-horizon setting as the effective discount factor  $\hat{d}_t$  converges to  $\gamma_m < 1$  as  $t \rightarrow \infty$ .

This formulation yields a practical algorithmic framework in which the agent learns a set of distributional value functions  $\{\eta^{\gamma_i}\}_{i=1}^m$ , each corresponding to an exponentially discounted problem. Notably, all predictions are conditioned on a single aggregate stock  $C_t^{\tilde{d}}$ , rather than maintaining separate stocks for each  $\gamma_i$ , since the policy is fully determined by the augmented state  $(s_t, C_t^{\tilde{d}})$ . At decision time  $t$ , given state  $(s_t, C_t^{\tilde{d}})$ , the agent uses the learned value distributions to reconstruct the distribution of the total outcome via (7). Then, for each action, it forms a mixture of the  $m$  exponential return distributions using the current weights  $w_{i,t}$  and selects the action that maximizes the objective functional  $K$ .

## 5 Extension to Infinite Horizon

While the theoretical guarantees for our backward induction algorithm in Section 3 rely on a finite horizon, extending them to the infinite-horizon setting requires additional structure. We therefore study a principled approximation scheme that enables performance guarantees under additional assumptions. To achieve this, we must analyze the asymptotic behavior of both the discount function and the objective function. In this section, we further assume that  $d_t$  converges to zero and is summable, i.e.,  $\lim_{t \rightarrow \infty} d_t = 0$ , and  $\sum_{t=0}^{\infty} d_t < \infty$  (e.g., requiring  $b > 1$  for generalized hyperbolic discounting of the form  $(1 + kt)^{-b}$ ).

### 5.1 Discount Function's Asymptotic Behavior

A primary challenge in applying general discounting to infinite-horizon problems is ensuring that the model remains well-posed. If the one-step discount factor  $\hat{d}_t$  converges to 1 as  $t \rightarrow \infty$ , as is the case with hyperbolic discounting, the Bellman operator fails to be a contraction. To address this, we require a discount function where the one-step factor asymptotically converges to a limit strictly less than one. We present one such construction method here, with an alternative approach detailed in Appendix F.1.

A straightforward approach to prevent the one-step discount factor from approaching one is to enforce a strict upper bound  $\gamma_{\text{tail}} < 1$ . By capping the original  $\hat{d}_t$ , we define a modified one-step discount factor  $\hat{d}_t^{\text{new}} \doteq \min(\hat{d}_t, \gamma_{\text{tail}})$ . The corresponding full discount function is then constructed as the product of these factors, i.e.,  $d_t^{\text{new}} = \prod_{k=0}^{t-1} \hat{d}_k^{\text{new}}$ . For instance, applying this to a hyperbolic discount function  $\hat{d}_t$  results in a  $\hat{d}_t^{\text{new}}$  that exhibits hyperbolic behavior initially before transitioning to standard exponential decay. This approach is equivalent to selecting a horizon  $T$  and bounding the one-step discount function by  $\hat{d}_T$ , a strategy we adopt in our infinite-horizon algorithm.

### 5.2 Objective Function's Asymptotic Behavior

Regarding the objective function, the following lemma demonstrates that for OCE objectives with a strictly increasing utility function, the associated optimal policy becomes risk-neutral as  $t \rightarrow \infty$ . We delegate the proof and discussion about non-smooth OCEs (such as CVaR) in Appendix F.2.

**Lemma 5.1** (Asymptotic Risk-Neutrality). *Let  $f$  be a strictly increasing, twice continuously differentiable utility function with bounded second derivative. Then, as  $t \rightarrow \infty$ , the value of any optimal action for the OCE objective induced by  $f$  converges to the value of an optimal action for the risk-neutral (expected value) objective.*

Now, we propose an approximate algorithm for the infinite-horizon case, inspired by the work of Hau et al. [2023] on entropic risk measures. The core idea is that as  $t \rightarrow \infty$ , the agent's risk preferences converge to risk-neutrality. This observation justifies considering a planning horizon with the general discounting and risk-sensitive policy, and approximating the problem beyond this point with a stationary, risk-neutral policy. The algorithmic procedure is described in Algorithm 1.

**Algorithm 1** Distributional VI for Infinite-Horizon MDPs with General Discounting

---

**Input:** Planning horizon  $T' < \infty$ , functional  $K$   
 $\triangleright // 1. Solve the stationary risk-neutral tail problem$   
 Set the effective discount factor  $\gamma_{\text{tail}} \leftarrow d_{T'+1}/d_{T'}$   
 Compute the optimal risk-neutral policy  $\pi_{\text{RN}}^*$  and its return distribution  $\eta^{\pi_{\text{RN}}^*}$  under discount  $\gamma_{\text{tail}}$   
 $\triangleright // 2. Perform finite-horizon backward induction$   
 Initialize terminal value distribution:  $\hat{\eta}_{T'}^*(\cdot) \leftarrow \eta^{\pi_{\text{RN}}^*}(\cdot)$   
**for**  $t = T' - 1$  **to** 0 **do**  
 Compute  $\hat{\eta}_t^* \leftarrow \mathcal{T}_*^d \hat{\eta}_{t+1}^*$  (Thm. 3.2)  
 Let  $\hat{\pi}_t^*$  be a greedy policy with respect to  $\hat{\eta}_{t+1}^*$   
**end for**  
 $\triangleright // 3. Construct and return the composite policy$   
 Construct the final policy  $\hat{\pi}^*$  such that

$$\hat{\pi}_t^* = \begin{cases} \hat{\pi}_t^* & \text{if } t < T' \\ \pi_{\text{RN}}^* & \text{if } t \geq T' \end{cases}$$

**Output:** An approximately optimal policy  $\hat{\pi}^*$

---

Having defined the approximation scheme, we can quantify the performance loss incurred by switching to a risk-neutral policy at the truncation horizon  $T'$ . While this approximation is applicable to any risk measure that exhibits asymptotic risk-neutrality, including Mean-CVaR with non-zero weight on Mean and Entropic Risk, we establish a convergence rate for the specific case of Entropic Risk. The following theorem provides an upper bound on the suboptimality of the policy  $\hat{\pi}^*$  for the inner optimization objective. This bound demonstrates that the error decays quadratically with the discount factor  $d_{T'}$ , ensuring that the approximation error vanishes rapidly as the planning horizon increases. By combining this result with a grid search over the initial stock  $c$ , following the derivation in Proposition 3.5, one recovers a total suboptimality bound for the full  $\text{OCE}_f$  objective. We refer to Appendix F.3 for details of the proof and a discussion regarding non-differentiable objectives.

**Theorem 5.2** (Performance Bound for Approximate Infinite-Horizon Policy). *Let the objective functional  $K$  be the Entropic Risk Measure with risk aversion coefficient  $\beta > 0$  (corresponding to the exponential utility  $f(x) = \beta^{-1}(1 - e^{-\beta x})$ ). Let the discount function  $d_t$  follow the truncation scheme with parameter  $\gamma_{\text{tail}} < 1$  for  $t \geq T'$ . Let  $\pi^*$  be the optimal non-stationary policy for the infinite-horizon problem,  $\hat{\pi}^*$  the policy returned by Algorithm 1 with planning horizon  $T'$ , and  $\Delta_G$  the range of the discounted returns. Then, the suboptimality of the approximate policy at time  $t = 0$  is bounded by*

$$\|F_K(\eta_0^{\pi^*}) - F_K(\eta_0^{\hat{\pi}^*})\|_\infty \leq \frac{d_{T'}^2 \cdot \beta \cdot \Delta_G^2}{8}.$$

## 6 Experiment Results

In this section, we design a series of experiments to evaluate the performance of our algorithm. Further details regarding the environments, hyperparameters, and expanded results are provided in Appendices G and H. The implementation code is available in the supplementary material.

### 6.1 Goal-Based Wealth Management

Inspired by the hypothetical scenario from Fedus et al. [2019] and the investment problem proposed by Schultheis et al. [2022], we devise a goal-based wealth management (GBWM) application, in which the agent must invest his or her wealth and determine when fulfilling specified goals over a long-term trading horizon. Das et al. [2022] developed a DP framework to explicitly solve a class of GBWM problems, while Das & Varma [2020] considered Q-learning for the one-goal GBWM problem and Dixon & Halperin [2020] used a probabilistic extension of Q-learning.

Consider an agent who can invest funds to achieve some financial goals in the future. Each goal  $\psi$  is characterized by a cost  $c_t(\psi)$  and a utility  $u_t(\psi)$  representing the agent's satisfaction from realizing the goal. The agent begins with an initial wealth  $y_0 \in \mathbb{R}_+$  and, at each period  $t \in \{0, \dots, T\}$ , makes two decisions: (i) which financial goal  $\psi_t \in \{0, \dots, \Psi_t\}$  to fulfill, and (ii) which investment portfolio  $\ell_t \in \{1, \dots, L\}$  to follow over the next period using the

remaining wealth?<sup>1</sup> At each period, the state is given by  $s_t = (t, y_t)$ , while the 2-tuple action  $a_t = (\psi_t, \ell_t)$  corresponds to the goals and portfolio strategy. State transitions occur in two stages, where we first deduct the cost of the selected goal  $y_{t+} = y_t - c_t(\psi_t)$  and then  $y_{t+1}$  is obtained by investing  $y_{t+}$  in the portfolio  $\ell_t$ . The reward is given by the goal's utility  $r(s_t, a_t) = u_t(\psi_t)$ . At the terminal time, one may include a final reward for the utility associated with remaining wealth  $u_T(y_T)$ , but it must be carefully designed to avoid hyper-sensitive policies.

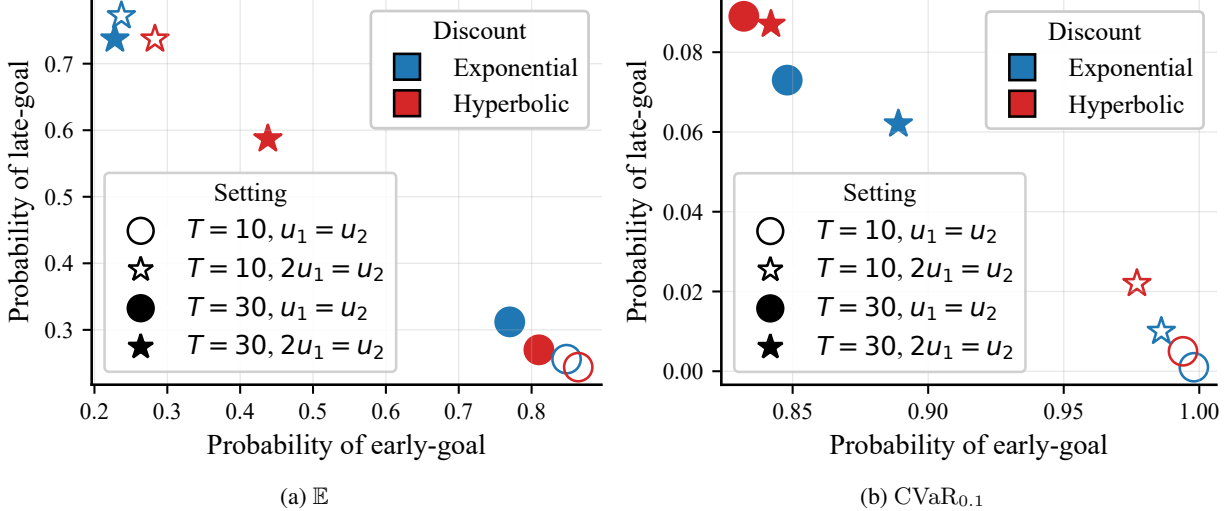


Figure 3: **The preference reversals in GBWM.** Monte-Carlo probabilities of achieving the two goals for a risk-neutral (Fig. 3a) and risk-sensitive (Fig. 3b) agent. Colors indicate the discounting approach, and shapes represent different environment settings.

In Figure 3, we show Monte-Carlo estimations of the probabilities of achieving the early-goal with cost  $c_{T/2}(1) = 100$  and late-goal with cost  $c_T(1) = 150$  under the optimal policy. Estimates are computed over 10,000 episodes and averaged across three different runs. We ran our algorithm with both exponential and hyperbolic discounting and observed that when the two goals have the same utility ( $u_{T/2}(1) = u_T(1) = 1000$ , circles), the agent accomplishes a goal if he or she has the wealth available, as there is no incentive in waiting. There is little to no difference for risk-neutral agents between a 10-period (hollow) or 30-period (filled) problem. We then compare these observations with the case where the late-goal is twice as valuable as the early-goal ( $u_{T/2}(1) = 1000, u_T(1) = 2000$ , stars). Then, the hyperbolic discounting displays substantially larger probabilities of achieving the first goal, visible as a shift of the red filled star relative to its exponential counterpart, reflecting the impatience and preference reversals of the agent. This shows that an exponentially discounted optimal policy fails to capture preference reversals, in a similar manner to the hypothetical scenario described in the introduction from Fedus et al. [2019].

For risk-sensitive agents, the chosen portfolios tend to be more conservative and typically support the purchase of a single goal, leading to smaller expected total utilities under the learned optimal policy. In fact, the preferences reversals are less pronounced compared to risk-neutral agents, where the strong risk-aversion drives the agent to secure a goal as soon as there is an opportunity, as observed by the large probabilities of achieving the early-goal in Figure 3b.

## 6.2 Atari 2600

To demonstrate scalability to high-dimensional state spaces, we evaluated our algorithm on the Atari 2600 suite [Bellemare et al., 2013]. To isolate the impact of time-consistency, we compare our time-consistent agent against the time-inconsistent baseline using identical architectures. Our objective is to verify that resolving this theoretical inconsistency improves performance, rather than to claim state-of-the-art results against standard exponential baselines. Agents were trained for 40 million frames. Although this is shorter than the standard 200 million, the budget was sufficient to reveal clear differences in policy quality between the approaches.

The results, summarized in Figure 4, demonstrate a clear advantage of the time-consistent approach across 50 Atari games. Averaged over three seeds per game, the time-consistent agent achieves a mean improvement of 39.89%

<sup>1</sup>For notational convenience, we assume that the trading horizon is discretized into a sequence of time steps with equal duration, the 15 candidate portfolios are ordered by risk aversion from conservative to aggressive as in Das et al. [2022], every period has a “no-goal” option with  $c_t(0) = u_t(0) = 0$ , and the agent can fulfil at most one goal.

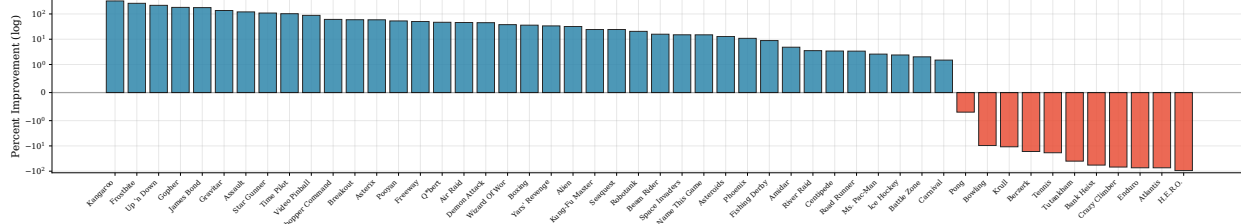


Figure 4: **Relative performance improvement of our Time-Consistent algorithm across 50 Atari games.** Each bar shows the percentage improvement in mean return for the Time-Consistent policy over the Time-Inconsistent baseline, averaged over 3 seeds per game. The Time-Consistent policy outperforms in 39 out of 50 games. Across all games, it achieves a mean improvement of 39.89% and a median improvement of 18.14%, demonstrating the benefits of maintaining time-consistency under hyperbolic discounting.

and a median improvement of 18.14% relative to the time-inconsistent baseline. This consistent performance gap indicates that the theoretical incoherence induced by enforcing stationarity under hyperbolic objectives is not merely conceptual, but a practical limitation that hinders learning in complex environments. To confirm that these gains stem from time-consistency rather than simply including time in the state, Appendix H.4 compares against a Time-Aware Time-Inconsistent agent. Our method retains a significant advantage under identical state information, confirming that the improvement arises from the time-consistent optimization objective.

## 7 Conclusion

In this paper, we introduced a unified framework for stock augmentation in distributional RL that supports agents with various time and risk preferences. Our approach accommodates general discount functions and OCE risk measures, outperforms prior precommitment RL algorithms with general discounting [Fedus et al., 2019], and captures preference reversals commonly observed in human behavior.

There are several promising directions for future work. First, agents could adaptively learn their own time preferences by optimizing multi-horizon weights, in a manner similar to meta-gradient reinforcement learning [Xu et al., 2018, Zahavy et al., 2020]. Beyond learning scalar time preferences, the multi-horizon framework also enables the optimization of multi-dimensional utility functions that capture complex trade-offs across timescales. Such objectives operate directly on the joint distribution of the multi-horizon return vector and therefore require learning the full joint return distribution [see e.g., Zhang et al., 2021, Wiltzer et al., 2024]. Together, these extensions move beyond approximating human-like discounting and open the door to agents with richer risk profiles for complex decision-making tasks.

## Acknowledgements

We thank the Digital Research Alliance of Canada (alliancecan.ca) for providing the computational resources used in this work. The second author also gratefully acknowledges support from the Natural Sciences and Engineering Research Council of Canada (grant PDF-2024-587484).

## References

- Amit, R., Meir, R., and Ciosek, K. Discount Factor as a Regularizer in Reinforcement Learning. In *Proceedings of the 37th International Conference on Machine Learning*, pp. 269–278. PMLR, 2020.
- Badia, A. P., Piot, B., Kapturowski, S., Sprechmann, P., Vitvitskyi, A., Guo, Z. D., and Blundell, C. Agent57: Outperforming the Atari Human Benchmark. In *Proceedings of the 37th International Conference on Machine Learning*, pp. 507–517. PMLR, 2020. URL <https://proceedings.mlr.press/v119/badia20a.html>.
- Bäuerle, N. and Glauner, A. Distributionally Robust Markov Decision Processes and Their Connection to Risk Measures. *Mathematics of Operations Research*, 2021. doi:10.1287/moor.2021.1187.
- Bäuerle, N. and Ott, J. Markov Decision Processes with Average-Value-at-Risk criteria. *Mathematical Methods of Operations Research*, 74(3):361–379, 2011. doi:10.1007/s00186-011-0367-0.
- Bäuerle, N. and Rieder, U. More Risk-Sensitive Markov Decision Processes. *Mathematics of Operations Research*, 39(1):105–120, 2014. doi:10.1287/moor.2013.0601.

Bayraktar, E., Huang, Y.-J., Wang, Z., and Zhou, Z. Relaxed Equilibria for Time-Inconsistent Markov Decision Processes. *Mathematics of Operations Research*, 2024. doi:10.1287/moor.2023.0209.

Bellemare, M. G., Naddaf, Y., Veness, J., and Bowling, M. The arcade learning environment: An evaluation platform for general agents. *Journal of Artificial Intelligence Research*, 47:253–279, jun 2013.

Bellemare, M. G., Dabney, W., and Munos, R. A Distributional Perspective on Reinforcement Learning. In *Proceedings of the 34th International Conference on Machine Learning*, pp. 449–458. PMLR, 2017.

Bellemare, M. G., Dabney, W., and Rowland, M. *Distributional Reinforcement Learning*. The MIT Press, 2023. ISBN 978-0-262-37402-6. doi:10.7551/mitpress/14207.001.0001.

Ben-Tal, A. and Teboulle, M. An Old-New Concept of Convex Risk Measures: The Optimized Certainty Equivalent. *Mathematical Finance*, 17(3):449–476, 2007. doi:10.1111/j.1467-9965.2007.00311.x.

Coache, A. and Jaimungal, S. Reinforcement learning with dynamic convex risk measures. *Mathematical Finance*, 34(2):557–587, 2024. doi:10.1111/mafi.12388.

Cox, J. C., Ingersoll, J. E., Ross, S. A., et al. A theory of the term structure of interest rates. *Econometrica*, 53(2):385–407, 1985.

Dabney, W., Rowland, M., Bellemare, M., and Munos, R. Distributional Reinforcement Learning With Quantile Regression. *Proceedings of the AAAI Conference on Artificial Intelligence*, 32(1), 2018. doi:10.1609/aaai.v32i1.11791.

Das, S. R. and Varma, S. Dynamic goals-based wealth management using reinforcement learning. *Journal Of Investment Management*, 18(2):1–20, 2020.

Das, S. R., Ostrov, D., Radhakrishnan, A., and Srivastav, D. Dynamic optimization for multi-goals wealth management. *Journal of Banking & Finance*, 140:106192, 2022.

Di Castro, D., Oren, J., and Mannor, S. Practical Risk Measures in Reinforcement Learning. *arXiv preprint arXiv:1908.08379*, 2019.

Dixon, M. and Halperin, I. G-Learner and GIRL: Goal Based Wealth Management with Reinforcement Learning. *arXiv preprint arXiv:2002.10990*, 2020.

Fedus, W., Gelada, C., Bengio, Y., Bellemare, M. G., and Larochelle, H. Hyperbolic Discounting and Learning over Multiple Horizons. *arXiv preprint arXiv:1902.06865*, 2019.

François-Lavet, V., Fonteneau, R., and Ernst, D. How to Discount Deep Reinforcement Learning: Towards New Dynamic Strategies. *arXiv preprint arXiv:1512.02011*, 2016.

Green, L. and Myerson, J. A discounting framework for choice with delayed and probabilistic rewards. *Psychological bulletin*, 130(5):769, 2004.

Hau, J. L., Petrik, M., and Ghavamzadeh, M. Entropic Risk Optimization in Discounted MDPs. In *Proceedings of The 26th International Conference on Artificial Intelligence and Statistics*, pp. 47–76. PMLR, 2023.

Huang, S., Dossa, R. F. J., Ye, C., Braga, J., Chakraborty, D., Mehta, K., and Araújo, J. G. M. CleanRL: High-quality Single-file Implementations of Deep Reinforcement Learning Algorithms. *Journal of Machine Learning Research*, 23(274):1–18, 2022. URL <http://jmlr.org/papers/v23/21-1342.html>.

Jaderberg, M., Mnih, V., Czarnecki, W. M., Schaul, T., Leibo, J. Z., Silver, D., and Kavukcuoglu, K. Reinforcement learning with unsupervised auxiliary tasks. *arXiv preprint arXiv:1611.05397*, 2016.

Lattimore, T. and Hutter, M. General time consistent discounting. *Theoretical Computer Science*, 519:140–154, 2014. doi:10.1016/j.tcs.2013.09.022.

Masset, P., Tano, P., Kim, H. R., Malik, A. N., Pouget, A., and Uchida, N. Multi-timescale reinforcement learning in the brain. *Nature*, pp. 1–9, 2025. doi:10.1038/s41586-025-08929-9.

Mnih, V., Kavukcuoglu, K., Silver, D., Rusu, A. A., Veness, J., Bellemare, M. G., Graves, A., Riedmiller, M., Fidjeland, A. K., Ostrovski, G., Petersen, S., Beattie, C., Sadik, A., Antonoglou, I., King, H., Kumaran, D., Wierstra, D., Legg, S., and Hassabis, D. Human-level control through deep reinforcement learning. *Nature*, 518(7540):529–533H, 2015. doi:10.1038/nature14236.

Moghimi, M. and Ku, H. Beyond CVaR: Leveraging Static Spectral Risk Measures for Enhanced Decision-Making in Distributional Reinforcement Learning. In *Forty-Second International Conference on Machine Learning*, 2025a.

Moghimi, M. and Ku, H. Risk-sensitive actor-critic with static spectral risk measures for online and offline reinforcement learning. *arXiv preprint arXiv:2507.03900*, 2025b.

Morimura, T., Sugiyama, M., Kashima, H., Hachiya, H., and Tanaka, T. Nonparametric return distribution approximation for reinforcement learning. In *Proceedings of the 27th International Conference on International Conference on Machine Learning*, ICML’10, pp. 799–806, Madison, WI, USA, 2010. Omnipress. ISBN 978-1-60558-907-7.

Naik, A., Shariff, R., Yasui, N., Yao, H., and Sutton, R. S. Discounted reinforcement learning is not an optimization problem. *arXiv preprint arXiv:1910.02140*, 2019.

Osogami, T. Robustness and risk-sensitivity in Markov decision processes. In *Advances in Neural Information Processing Systems*, volume 25. Curran Associates, Inc., 2012.

Pardo, F., Tavakoli, A., Levdik, V., and Kormushev, P. Time Limits in Reinforcement Learning. In *Proceedings of the 35th International Conference on Machine Learning*, pp. 4045–4054. PMLR, 2018.

Petrik, M. and Scherrer, B. Biasing approximate dynamic programming with a lower discount factor. *Advances in Neural Information Processing Systems*, 21, 2008.

Pires, B. Á., Rowland, M., Borsa, D., Guo, Z. D., Khetarpal, K., Barreto, A., Abel, D., Munos, R., and Dabney, W. Optimizing Return Distributions with Distributional Dynamic Programming. *arXiv preprint arXiv:2501.13028*, 2025. doi:10.48550/arXiv.2501.13028.

Pitis, S. Rethinking the Discount Factor in Reinforcement Learning: A Decision Theoretic Approach. *Proceedings of the AAAI Conference on Artificial Intelligence*, 33(01):7949–7956, 2019. doi:10.1609/aaai.v33i01.33017949.

Ruszczyński, A. Risk-averse dynamic programming for Markov decision processes. *Mathematical Programming*, 125(2):235–261, 2010. doi:10.1007/s10107-010-0393-3.

Schultheis, M., Rothkopf, C. A., and Koepll, H. Reinforcement Learning with Non-Exponential Discounting. *Advances in Neural Information Processing Systems*, 35:3649–3662, 2022.

Tamar, A., Di Castro, D., and Mannor, S. Policy gradients with variance related risk criteria. In *Proceedings of the 29th International Conference on International Conference on Machine Learning*, ICML’12, pp. 1651–1658, Madison, WI, USA, 2012. Omnipress. ISBN 978-1-4503-1285-1.

Tamar, A., Chow, Y., Ghavamzadeh, M., and Mannor, S. Sequential Decision Making With Coherent Risk. *IEEE Transactions on Automatic Control*, 62(7):3323–3338, 2017. doi:10.1109/TAC.2016.2644871.

Vasicek, O. An equilibrium characterization of the term structure. *Journal of Financial Economics*, 5(2):177–188, 1977.

Von Neumann, J. and Morgenstern, O. Theory of games and economic behavior: 60th anniversary commemorative edition. In *Theory of Games and Economic Behavior*. Princeton university press, 2007.

White, M. Unifying Task Specification in Reinforcement Learning. In *Proceedings of the 34th International Conference on Machine Learning*, pp. 3742–3750. PMLR, 2017.

Wiltzer, H., Farebrother, J., Gretton, A., and Rowland, M. Foundations of Multivariate Distributional Reinforcement Learning. In *The Thirty-eighth Annual Conference on Neural Information Processing Systems*, 2024.

Xu, Z., van Hasselt, H. P., and Silver, D. Meta-Gradient Reinforcement Learning. In *Advances in Neural Information Processing Systems*, volume 31. Curran Associates, Inc., 2018.

Zahavy, T., Xu, Z., Veeriah, V., Hessel, M., Oh, J., van Hasselt, H. P., Silver, D., and Singh, S. A Self-Tuning Actor-Critic Algorithm. In *Advances in Neural Information Processing Systems*, volume 33, pp. 20913–20924. Curran Associates, Inc., 2020.

Zhang, P., Chen, X., Zhao, L., Xiong, W., Qin, T., and Liu, T.-Y. Distributional Reinforcement Learning for Multi-Dimensional Reward Functions. In *Advances in Neural Information Processing Systems*, volume 34, pp. 1519–1529. Curran Associates, Inc., 2021.

## A Related Work

**General Discounting in RL.** Many RL frameworks primarily apply an exponential discount factor as a regularization tool to ensure convergence and stabilize training. This choice, however, imposes structural constraints on how future rewards are discounted, limiting the modeling expressiveness of the resulting algorithms. Furthermore, alternative discounting schemes naturally appear in stochastic environments and model-based settings. For instance, we show in Appendix B that, under some model assumptions, the risk-neutral expectation of the price of a zero-coupon bond leads to a deterministic hyperbolic discount function. These considerations motivated the development of RL frameworks that admit more general discounting mechanisms beyond the exponential form.

One major approach redefines the discount function to be explicitly time-dependent. Lattimore & Hutter [2014] provide a complete characterization of time consistency within this model, proving that a policy remains consistent if and only if the agent’s relative preferences for future rewards remain constant over its lifetime. Another line of research treats the discount factor as an adaptive parameter, to be tuned via meta-learning [Xu et al., 2018, Zahavy et al., 2020] or adjusted dynamically to improve training stability [François-Lavet et al., 2016]. A third, more foundational approach provides a formal basis for agents to have state- and action-dependent discount rates [White, 2017, Pitis, 2019].

Within this landscape, several distinct paradigms for handling general discounting have emerged. Fedus et al. [2019] proposed a practical, bottom-up approach to approximate hyperbolic discounting by aggregating the value functions of multiple agents, each with a different exponential discount factor. In contrast, Schultheis et al. [2022] developed a theoretically principled, top-down model that embraces the time-dependency of the problem, leading to a non-stationary optimal policy. Taking a different path, Bayraktar et al. [2024] re-framed the issue as a game-theoretic problem between an agent’s present and future selves, solving for a stable (but not necessarily  $t_0$ -optimal) equilibrium policy. Our work builds most directly on the principled, time-dependent optimal control paradigm.

To be comprehensive, we mention that the average-reward formulation, which optimizes the long-run reward per time-step, offers another possible approach for long-horizon problems. We do not take this approach, however, because it creates a mismatch when the goal is to optimize a utility function (under the expected theory [Von Neumann & Morgenstern, 2007]) over total accumulated return. A static utility function  $f(G)$ , meant to evaluate the risk profile of the total return distribution, is conceptually incompatible with an objective based on per-step averages.

**Risk-Sensitive RL.** Properly accounting for risk preferences of the agent is as crucial as accounting for time preferences. In many real-life applications such as resource management, financial investment or healthcare decision-making, ignoring environmental uncertainty can cause catastrophic outcomes. A large body of work in risk-sensitive RL has sought to move beyond expectation-based goal functionals. Many contributions have focused on classes of static risk measures [see e.g., Bäuerle & Ott, 2011, Tamar et al., 2012, Di Castro et al., 2019], while others have investigated robust Markov decision processes for optimizing worst-case expectations [see e.g., Osogami, 2012].

Parallel to these developments, distributional RL [Morimura et al., 2010, Bellemare et al., 2017] provided a framework for modeling the full (discounted) return distribution, allowing agents to capture parametric uncertainty and optimize risk-sensitive objectives with more stable learning algorithms. Our work falls in the realm of these works. Alternatively, a class of dynamic risk measures has been developed to ensure time-consistency by construction [see e.g. Ruszczyński, 2010], for which many authors have constructed time-consistent RL algorithms [see e.g. Tamar et al., 2017, Coache & Jaimungal, 2024]. These alternative works, however, fall outside the scope of our work with their limited interpretability.

**Time-Consistency and State Augmentation.** An agent is considered time-consistent if the optimal plan it formulates at the beginning of an episode remains optimal at all future decision points. However, when an agent’s preferences are not based on simple expected returns with exponential discounting, this property is often lost, leading to policies that are dynamically unstable. The literature has converged on state augmentation as the primary mechanism to restore tractability and consistency, and this augmentation serves two distinct but related purposes.

The first role of state augmentation is to make the problem amenable to standard DP techniques, especially when the optimal policy depends on the entire history of past rewards, making the search space of policies intractable. Bäuerle & Ott [2011] first introduced the concept of a stock to solve the CVaR optimization problem, demonstrating that the search for an optimal policy could be reduced from the space of history-dependent policies to the much smaller space of Markov policies defined on an augmented state space that tracks accumulated past costs. This powerful idea was later extended to the optimization of more general expected utility functions [Bäuerle & Rieder, 2014] and spectral risk measures [Bäuerle & Glauner, 2021], and related notions such as “time-awareness” state augmentation have been shown to improve policy stability in RL [Pardo et al., 2018]. The second, more conceptual role of state augmentation is to serve as an anytime proxy for the initial return distribution [Moghimi & Ku, 2025a,b, Pires et al., 2025]. Static utility and risk measures are, by definition, functionals of the entire distribution of returns as seen from the initial time step.

To make a decision at any future time that remains consistent with the initial objective, the agent requires information about how its current actions will affect that original distribution, which is exactly what the stock provides.

## B Discounting in Financial Applications

In many RL applications, the discount factor is primarily a regularization tool, introduced to ensure convergence and stabilize training, and its value is often tuned as a hyperparameter. However, in domains like finance, the discount factor has a precise economic meaning: it represents the present value of future risk-free cash flows, which is governed by the term structure of interest rates. While prior work, such as Fedus et al. [2019], has explored various discount functions derived from hazard priors, the direct connection of these functions to financial models is unclear.

In finance, the short-term interest rate is often modeled as a stochastic process. To derive a discount function, we consider the price of a zero-coupon bond at time  $t$ , denoted by  $P(t, T)$ , which pays \$1 at a future maturity date  $T > t$ . This price represents the value of a guaranteed dollar at time  $T$ , and is related to the path of the instantaneous short-rate, denoted by  $(r_u)_{u \in (t, T)}$ . Under no-arbitrage conditions, this price is given by the risk-neutral expectation of the discounted payoff:

$$P(t, T) = \mathbb{E} \left[ e^{- \int_t^T r_u du} \right].$$

Our deterministic discount function from the perspective of time zero is precisely the price of a zero-coupon bond that matures at time  $t$ , i.e.,  $d_t \equiv P(0, t)$ . If the interest rate process  $r_u$  is guaranteed to be non-negative, then the integral is non-negative and thus  $d_t < 1$  for  $t > 0$ , in line with our non-increasing assumption on the discount factor.

Seminal models from Vasicek [1977] or Cox-Ingersoll-Ross (CIR) [Cox et al., 1985] provide analytic solutions for this bond price. The CIR model describes the evolution of  $r_t$  as

$$dr_t = a(b - r_t)dt + \sigma \sqrt{r_t} dW_t,$$

where  $a$  is the speed of mean reversion,  $b$  is the long-term mean rate,  $\sigma$  is the volatility, and  $dW_t$  is a Wiener process. The CIR model guarantees non-negative interest rates as long as  $2ab \geq \sigma^2$ . In this case, the bond price has an affine term structure solution of the form  $P(t, T) = A(t, T)e^{-B(t, T)r_t}$ , where the functions  $A(t, T)$  and  $B(t, T)$  depend only on the time to maturity  $\tau \doteq T - t$  and  $h \doteq \sqrt{a^2 + 2\sigma^2}$ :

$$A(t, T) = \left[ \frac{2he^{(a+h)\tau/2}}{(a+h)(e^{h\tau} - 1) + 2h} \right]^{2ab/\sigma^2} \quad \text{and} \quad B(t, T) = \frac{2(e^{h\tau} - 1)}{(a+h)(e^{h\tau} - 1) + 2h}.$$

The general nature of  $d_t$  in our model provides the flexibility to choose a discount function that is well-motivated by the specific application domain. To obtain our discount function in the CIR model, we set  $t = 0$  and  $T = t$  (and thus  $\tau = t$ ), which yields  $d_t = A(0, t)e^{-B(0, t)r_0}$ . We provide a comparison of various discounting approaches in Figure 5. Besides this CIR model, other methods can be used for modeling time preference, such as deriving the discount function directly from a hazard rate model. Our framework is sufficiently general to accommodate such choices, providing a principled foundation for risk-sensitive decision-making under sophisticated and realistic models of time.

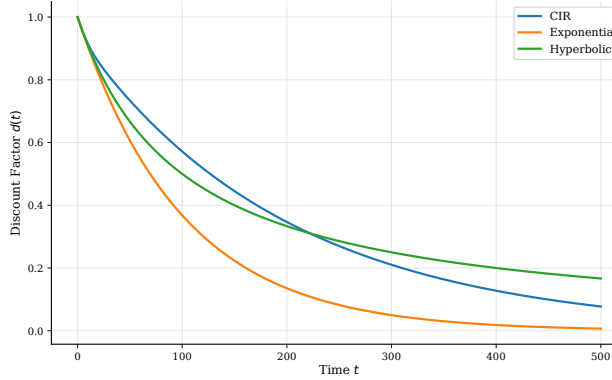


Figure 5: **From interest rates to discount functions.** Comparison of exponential with  $\gamma = 0.99$  (Orange), hyperbolic with  $k = 0.01$  (Green), and CIR-based discount factors with parameters  $a = 0.05$ ,  $b = 0.01$ ,  $\sigma = 0.1$ , and  $r_0 = 0.01$  (Blue)

## C Anytime Proxy

In this section, we provide the derivations for the “anytime proxy” relationships. In the case of exponential discounting, we recover (2) as follows:

$$\begin{aligned}
 C_0^\gamma + G_0^\gamma &= C_0^\gamma + \sum_{k=0}^{\infty} \gamma^k R_{k+1} \\
 &= C_0^\gamma + \sum_{k=0}^{t-1} \gamma^k R_{k+1} + \sum_{k=t}^{\infty} \gamma^k R_{k+1} \\
 &= C_0^\gamma + \sum_{k=0}^{t-1} \gamma^k R_{k+1} + \gamma^t \sum_{k=0}^{\infty} \gamma^k R_{t+k+1} \\
 &= \gamma^t \left( \frac{C_0^\gamma + \sum_{k=0}^{t-1} \gamma^k R_{k+1}}{\gamma^t} + \sum_{k=0}^{\infty} \gamma^k R_{t+k+1} \right) \\
 &= \gamma^t (C_t^\gamma + G_t^\gamma). \tag{8}
 \end{aligned}$$

Equation (4) for general discounting is given by

$$\begin{aligned}
 C_0^d + G_0^d &= C_0^d + \sum_{k=0}^{T-1} d_k R_{k+1} \\
 &= \left( C_0^d + \sum_{k=0}^{t-1} d_k R_{k+1} \right) + \sum_{k=t}^{T-1} d_k R_{k+1} \\
 &= d_t C_t^d + d_t \sum_{k=0}^{T-t-1} \frac{d(t+k)}{d_t} R_{t+k+1} \\
 &= d_t (C_t^d + G_t^d). \tag{9}
 \end{aligned}$$

For (7) as described in the multi-horizon setting, we have

$$\begin{aligned}
 C_0^{\tilde{d}} + G_0^{\tilde{d}} &= \tilde{d}_t C_t^{\tilde{d}} + \tilde{d}_t \sum_{k=0}^{T-t-1} \frac{\tilde{d}(t+k)}{\tilde{d}_t} R_{t+k+1} \\
 &= \tilde{d}_t C_t^{\tilde{d}} + \tilde{d}_t \sum_{k=0}^{T-t-1} \frac{\sum_{i=1}^m w_i \gamma_i^{t+k}}{\tilde{d}_t} R_{t+k+1} \\
 &= \tilde{d}_t C_t^{\tilde{d}} + \tilde{d}_t \sum_{i=1}^m \frac{w_i \gamma_i^t}{\tilde{d}_t} \sum_{k=0}^{T-t-1} \gamma_i^k R_{t+k+1} \\
 &= \tilde{d}_t \left( C_t^{\tilde{d}} + \sum_{i=1}^m w_{i,t} G_t^{\gamma_i} \right). \tag{10}
 \end{aligned}$$

## D OCE Utility Functions

The formulas for utility functions depicted in Figure 2 are presented in Table 1.

## E Proofs in Finite-Horizon Setting

### E.1 Time-Dependent Monotonicity Lemma

**Lemma E.1** (Time-Dependent Monotonicity (Restated)). *Let  $K$  be an objective functional satisfying the indifference to mixture property. For any time  $t < T$ , let  $\eta_{t+1}$  and  $\eta'_{t+1}$  be two return distribution functions for time  $t+1$ . If  $F_K \eta_{t+1} \geq F_K \eta'_{t+1}$ , then for any time- $t$  policy  $\pi_t$ :  $F_K(\mathcal{T}_{\pi_t}^d \eta_{t+1}) \geq F_K(\mathcal{T}_{\pi_t}^d \eta'_{t+1})$ .*

Table 1: Common Risk Measures as OCEs.

RISK NAME	PARAMETER	FORMULA	UTILITY FUNCTION $f(x)$
MEAN	NONE	$\mathbb{E}[G]$	$x$
CVAR	$\tau \in (0, 1]$	$\text{CVaR}_\tau(G)$	$\tau^{-1}(x)_-$
MEAN-CVAR	$\kappa_1 \in [0, 1]$ $\tau \in (0, 1]$	$\kappa_1 \mathbb{E}[G] + (1 - \kappa_1) \cdot \text{CVaR}_\tau(G)$	$\kappa_1(x)_+ + \kappa_2(x)_-, \text{ WHERE}$ $\kappa_2 = \tau^{-1}(1 - \kappa_1) + \kappa_1$
ENTROPIC RISK	$\beta \in (-\infty, 0)$	$\text{Entr}_\beta(G)$	$\frac{1}{\beta}(\exp(\beta x) - 1)$
MEAN-VARIANCE	$\kappa \in (0, \infty)$	$\mathbb{E}[G] - \kappa \cdot \text{Var}(G)$	$(x - \kappa x^2) \mathbb{I}\{x \leq \frac{1}{2\kappa}\}$ $+ \frac{1}{4\kappa} \mathbb{I}\{x > \frac{1}{2\kappa}\}$

*Proof.* The proof adapts Lemma 14 in Pires et al. [2025]. We fix a policy  $\pi_t$  and state  $(s, c) \in \mathcal{S} \times \mathcal{C}$ . The hypothesis  $F_K \eta_{t+1} \geq F_K \eta'_{t+1}$  implies that for any realization of the next state and stock  $(s', c')$ , we have  $K \text{df}(d_{t+1} c' + d_{t+1} G) \geq K \text{df}(d_{t+1} c' + d_{t+1} G')$ , where  $G \sim \eta_{t+1}(s', c')$  and  $G' \sim \eta'_{t+1}(s', c')$ .

Using the recursive definitions of the stock update and the Bellman operator, the total unscaled outcome at time  $t$  satisfies the identity:

$$d_t c + d_t (R_{t+1} + \hat{d}_t G) \stackrel{\mathcal{D}}{=} d_{t+1} C_{t+1}^d + d_{t+1} G.$$

This reveals that the random variable evaluated by  $K$  at time  $t$  is a probabilistic mixture (over  $S_{t+1}, R_{t+1}$ ) of the random variables evaluated at time  $t+1$ . Since the preference holds component-wise for every realization, the Indifference to Mixtures property in Definition 2.2 ensures the preference is preserved for the mixture, proving the lemma.  $\square$

## E.2 Optimality of Distributional Backward Induction

**Theorem E.2** (Optimality of Distributional Backward Induction (Restated)). *Let the problem horizon  $T \in \mathbb{N}$  be finite and known, and let the objective functional  $K$  be indifferent to mixtures. Assume that the sequence of return distributions  $\eta^* = (\eta_0^*, \dots, \eta_T^*)$  is generated by the following backward induction algorithm:*

- **Base Case:** For all  $(s, c) \in \mathcal{S} \times \mathcal{C}$ , set  $\eta_T^*(s, c) = \delta_0$ .
- **Recursive Step:** For  $t = T-1$  down to 0, compute  $\eta_t^* \doteq \mathcal{T}_*^d \eta_{t+1}^*$ , where  $\mathcal{T}_*^d$  is the greedy time-dependent distributional Bellman operator, defined such that for any function  $\eta_{t+1}$  and for all  $(s, c) \in \mathcal{S} \times \mathcal{C}$ , it returns the function  $\eta_t$  satisfying:

$$(F_K \eta_t)(s, c) = \sup_{\pi_t} (F_K(\mathcal{T}_{\pi_t}^d \eta_{t+1}))(s, c).$$

Then, the sequence  $\eta^*$  is a sequence of optimal return distributions. Furthermore, the non-stationary policy  $\pi^* = (\pi_0^*, \dots, \pi_{T-1}^*)$ , where each  $\pi_t^*$  is a greedy policy with respect to  $\eta_{t+1}^*$ , is optimal.

*Proof.* The proof proceeds by backward induction on the time step  $t$ . **Base Case:** The theorem holds trivially at  $t = T$ . At the horizon,  $G_T^d = 0$ , so the optimal return from any state  $(s, c)$  and time  $T$  is deterministically zero, hence  $\eta_T^*(s, c) = \delta_0$  is the optimal return distribution function. **Recursive Step:** Assume that for some time step  $t+1 \in \{1, \dots, T\}$ ,  $\eta_{t+1}^*$  is the optimal return distribution function for any subproblem starting at or after time  $t+1$ . We aim to show that  $\eta_t^* \doteq \mathcal{T}_*^d \eta_{t+1}^*$  is optimal at time  $t$ . Let  $\pi_t^*$  be a greedy policy w.r.t.  $\eta_{t+1}^*$ . Consider an arbitrary policy  $\pi_{\geq t} = (\pi_t, \pi_{\geq t+1})$ . Its return distribution is  $\eta^{\pi_{\geq t}} = \mathcal{T}_{\pi_t}^d \eta^{\pi_{\geq t+1}}$ . By the inductive hypothesis,  $F_K \eta_{t+1}^* \geq F_K \eta^{\pi_{\geq t+1}}$ . Applying the Time-Dependent Monotonicity Lemma gives  $F_K(\mathcal{T}_{\pi_t}^d \eta_{t+1}^*) \geq F_K(\mathcal{T}_{\pi_t}^d \eta^{\pi_{\geq t+1}}) = F_K \eta^{\pi_{\geq t}}$ . By definition of the greedy operator,  $F_K \eta_t^* \geq F_K(\mathcal{T}_{\pi_t}^d \eta_{t+1}^*)$ . Chaining these inequalities yields  $F_K \eta_t^* \geq F_K \eta^{\pi_{\geq t}}$ . Since  $\pi_{\geq t}$  was arbitrary,  $\eta_t^*$  is optimal.  $\square$

## E.3 OCE Optimality Bound

**Proposition E.3** (OCE Optimality Bound (Restated)). *Let  $f : \mathbb{R} \rightarrow \mathbb{R}$  be an  $L$ -Lipschitz utility function. Let  $\pi^*$  be the optimal policy from Theorem 3.2, and let  $\hat{\pi}$  be the policy derived from an approximate backward induction with one-step errors  $(\varepsilon_0, \dots, \varepsilon_{T-1})$ . Let the outer optimization be performed over a finite grid  $\bar{\mathcal{C}}$  with spacing  $\delta$ . If  $\hat{c} \in \bar{\mathcal{C}}$  is the initial stock selected by the algorithm, the total suboptimality is bounded by:*

$$\text{OCE}_f(\eta_0^*) - (-\hat{c} + \mathbb{E}[f(\hat{c} + G^{\hat{\pi}})]) \leq 2\mathcal{E}_{DP} + \frac{(1+L)\delta}{2},$$

where  $\mathcal{E}_{DP} \doteq L \sum_{t=0}^{T-1} d_t \varepsilon_t$  is the cumulative DP error term.

*Proof.* The proof proceeds in three steps: deriving the inner approximation error, establishing the properties of the outer objective, and combining them into a total error bound.

**Step 1 – Inner DP Error Derivation.** Let  $\hat{\eta}_t = \mathcal{A}(\mathcal{T}_*^d \hat{\eta}_{t+1})$  be the return distribution computed by the approximate backward induction, where  $\mathcal{A}$  is an approximation operator. We define the cumulative estimation error in the Wasserstein metric as  $E_t \doteq \sup_{s,c} w(\eta_t^*(s, c), \hat{\eta}_t(s, c))$ . Given the one-step approximation error  $\varepsilon_t \doteq \sup_{s,c} w((\mathcal{T}_*^d \hat{\eta}_{t+1})(s, c), \hat{\eta}_t(s, c))$ , this error propagates according to the recursion:

$$\begin{aligned} E_t &\leq \sup_{s,c} [w(\mathcal{T}_*^d \eta_{t+1}^*, \mathcal{T}_*^d \hat{\eta}_{t+1}) + w(\mathcal{T}_*^d \hat{\eta}_{t+1}, \mathcal{A}(\mathcal{T}_*^d \hat{\eta}_{t+1}))] \\ &\leq \hat{d}_t \sup_{s',c'} w(\eta_{t+1}^*(s', c'), \hat{\eta}_{t+1}(s', c')) + \varepsilon_t \\ &= \hat{d}_t E_{t+1} + \varepsilon_t. \end{aligned}$$

Unrolling this recursion from  $E_T = 0$  yields  $E_0 \leq \sum_{t=0}^{T-1} d_t \varepsilon_t$ . Since  $F_K = U_f$  is  $L$ -Lipschitz, the error in the value function is bounded by  $\|U_f \eta_0^* - U_f \hat{\eta}_0\|_\infty \leq L E_0 = \mathcal{E}_{DP}$ . Furthermore, we must account for the performance of the policy  $\hat{\pi}$  actually derived from these approximate distributions. The true return distribution  $\eta_0^{\hat{\pi}}$  differs from the estimate  $\hat{\eta}_0$  due to the same accumulation of errors during greedy selection. Thus,  $\|U_f \hat{\eta}_0 - U_f \eta_0^{\hat{\pi}}\|_\infty \leq \mathcal{E}_{DP}$ .

**Step 2 – Outer Objective Properties.** Let  $J(c) \doteq -c + (U_f \eta_0^*)(s_0, c)$  be the true outer objective and  $\hat{J}(c) \doteq -c + (U_f \hat{\eta}_0)(s_0, c)$  be the approximate objective used by the algorithm. From Step 1, we have the uniform bound  $\sup_c |J(c) - \hat{J}(c)| \leq \mathcal{E}_{DP}$ . We also establish the Lipschitz continuity of the outer objective. Since  $f$  is  $L$ -Lipschitz, the expected utility term is  $L$ -Lipschitz with respect to  $c$ . Including the linear term  $-c$ ,  $J(c)$  is thus  $(1+L)$ -Lipschitz.

**Step 3 – Total Error Decomposition.** Let  $c^*$  be the global maximizer of  $J(c)$  (i.e., the true optimal stock) and  $\hat{c}$  be the maximizer of  $\hat{J}(c)$  on the grid  $\bar{\mathcal{C}}$  (i.e., the selected stock). Let  $c_{grid}^*$  be the point in  $\bar{\mathcal{C}}$  closest to  $c^*$ , such that  $|c^* - c_{grid}^*| \leq \delta/2$ . We decompose the total optimality gap, noting that the true value of the learned policy is  $J^{\hat{\pi}}(\hat{c}) \doteq -\hat{c} + \mathbb{E}[f(\hat{c}) + G^{\hat{\pi}}]$ :

$$\begin{aligned} \text{Gap} &= J(c^*) - J^{\hat{\pi}}(\hat{c}) \\ &= \underbrace{J(c^*) - J(c_{grid}^*)}_{\text{Discretization}} + \underbrace{J(c_{grid}^*) - \hat{J}(c_{grid}^*)}_{\text{Estimation Error}} + \underbrace{\hat{J}(c_{grid}^*) - \hat{J}(\hat{c})}_{\text{Optimization}} + \underbrace{\hat{J}(\hat{c}) - J^{\hat{\pi}}(\hat{c})}_{\text{Policy Performance Gap}} \\ &\leq (1+L) \frac{\delta}{2} + \mathcal{E}_{DP} + 0 + \mathcal{E}_{DP} \\ &= 2\mathcal{E}_{DP} + (1+L) \frac{\delta}{2}. \end{aligned}$$

The third term is  $\leq 0$  because  $\hat{c}$  maximizes  $\hat{J}$  over the grid. The fourth term applies the bound derived in Step 1 to the specific stock  $\hat{c}$ .  $\square$

## F Infinite-Horizon Setting

### F.1 Modified Integral Representation

A second method is to modify the integral representation of the discount function. As shown in Fedus et al. [2019], some discount functions, including hyperbolic, can be expressed as an integral of exponential functions over the discount factor  $\gamma \in [0, 1]$ :

$$d_t = \int_{\gamma=0}^1 w(\gamma) \gamma^t d\gamma.$$

For hyperbolic discounting,  $w(\gamma) = \frac{1}{k} \gamma^{1/k-1}$ . The convergence of  $\hat{d}_t$  to 1 is a direct consequence of the integration limit including  $\gamma = 1$ . By simply reducing the upper limit of integration to  $\gamma_{tail} < 1$ , we can construct a new discount function that excludes this problematic point. Solving this integral yields:

$$\int_{\gamma=0}^{\gamma_{tail}} \frac{1}{k} \gamma^{1/k-1} d\gamma = \left[ \frac{\gamma^{1/k-1}}{1-kt} \right]_0^{\gamma_{tail}} = \frac{\gamma_{tail}^{1/k-1}}{kt+1}.$$

To ensure the standard normalization  $d_0 = 1$ , we can normalize this function by its value at  $t = 0$ , which is  $\gamma_{\text{tail}}^{1/k}$ . This gives the final discount function:

$$d_t^{\text{new}} = \frac{\gamma_{\text{tail}}^t}{1 + kt}.$$

This function retains a hyperbolic-like character due to the  $1/(kt + 1)$  term, but its asymptotic behavior is now governed by the exponential term. The one-step discount factor is  $\hat{d}_t^{\text{new}} = \gamma_{\text{tail}}^k \cdot \frac{kt+1}{kt+k+1}$ , and its limit is  $\gamma_{\text{tail}}$ .

## F.2 Asymptotic Risk-Neutrality

**Lemma F.1** (Asymptotic Risk-Neutrality (Restated)). *Let  $f$  be a strictly increasing, twice continuously differentiable utility function with bounded second derivative. Then, as  $t \rightarrow \infty$ , the value of any optimal action for the OCE objective induced by  $f$  converges to the value of an optimal action for the risk-neutral (expected value) objective.*

*Proof of Lemma 5.1.* From (4), the total return can be expressed as  $d_t c_t + d_t G_t$ . The term  $d_t c_t = C_0 + \sum_{k=0}^{t-1} d_k R_{k+1}$  represents the unscaled accumulated rewards up to time  $t - 1$  and is constant with respect to the action  $a_t$ . The decision-dependent term is  $d_t G_t$ .

The agent's objective is to maximize  $\mathbb{E}[f(d_t c_t + d_t G_t)]$ . As  $t \rightarrow \infty$ , our assumption on the discount function is that  $d_t \rightarrow 0$ . We further assume that the utility function  $f$  has a bounded second derivative, i.e.,  $|f''(x)| \leq M$  for some constant  $M$ . We perform a second-order Taylor expansion of  $f$  around the constant term  $d_t c_t$ :

$$f(d_t c_t + d_t G_t) = f(d_t c_t) + f'(d_t c_t) d_t G_t + \frac{1}{2} f''(\xi) (d_t G_t)^2, \quad (11)$$

where  $\xi$  lies between  $d_t c_t$  and  $d_t c_t + d_t G_t$ . Taking the expectation, we obtain:

$$\mathbb{E}[f(d_t c_t + d_t G_t)] = f(d_t c_t) + f'(d_t c_t) d_t \mathbb{E}[G_t] + \mathcal{R}_t, \quad (12)$$

where the remainder term satisfies  $|\mathcal{R}_t| \leq \frac{1}{2} M d_t^2 \mathbb{E}[G_t^2]$ .

Since  $f(d_t c_t)$  is constant with respect to the action choice at time  $t$ , and  $f'(d_t c_t) > 0$  (strictly increasing utility) and  $d_t > 0$ , maximizing the objective is equivalent to maximizing the normalized expression:

$$\frac{\mathbb{E}[f(d_t c_t + d_t G_t)] - f(d_t c_t)}{d_t f'(d_t c_t)} = \mathbb{E}[G_t] + \frac{\mathcal{R}_t}{d_t f'(d_t c_t)}. \quad (13)$$

Analyzing the error term, we have:

$$\left| \frac{\mathcal{R}_t}{d_t f'(d_t c_t)} \right| \leq \frac{M d_t^2 \mathbb{E}[G_t^2]}{2 d_t f'(d_t c_t)} = \frac{M \mathbb{E}[G_t^2]}{2 f'(d_t c_t)} \cdot d_t. \quad (14)$$

Since returns are bounded,  $\mathbb{E}[G_t^2]$  is finite. As  $t \rightarrow \infty$ ,  $d_t \rightarrow 0$ , causing the error term to vanish. Consequently, the objective converges to maximizing  $\mathbb{E}[G_t]$ , implying the optimal policy becomes effectively risk-neutral.

□

## F.3 Performance Bound for Approximate Infinite-Horizon Policy

Our analysis is inspired by the work of Hau et al. [2023] on entropic risk measures. However, their approach leverages the specific factorization properties of the entropic measure. Our framework considers more general discount functions using distributional value functions. It also uses the stock-augmented space, which allows us to employ a similar proof technique for both the entropic risk measure (with twice-differentiable utility function) and the mean-CVaR (non-smooth utility function).

For the derivation of the performance bound, we utilize the specific certainty-equivalent form  $V_t(s, c)$  defined below. We note that under the assumption that the utility function  $f$  is strictly increasing, optimizing this formulation yields the exact same greedy policies as the objective  $F_K \eta_t^\pi$ . This is because the inverse function  $f^{-1}$  is strictly monotonic, and the subsequent subtraction of  $d_t c$  and scaling by  $1/d_t$  represent affine transformations that are constant with respect to the decision at time  $t$ . Thus, the preference ordering over actions remains invariant.

**Lemma F.2** (Lower Bound for the Certainty Equivalent Value Function). *Let the value function at time  $t$  for a state  $s \in \mathcal{S}$  and scaled stock  $c \in \mathcal{C}$  be defined as*

$$V_t(s, c) \doteq \frac{1}{d_t} (f^{-1}(\mathbb{E}[f(d_t c + d_t G_t(s, c))]) - d_t c),$$

where  $d_t > 0$  is the discount factor, and  $G_t(s, c)$  is a bounded random variable with support  $[G_{\min}, G_{\max}]$  representing future returns, where  $G_{\min} = R_{\min} \sum_{k=0}^{\infty} d_k$ , and  $G_{\max} = R_{\max} \sum_{k=0}^{\infty} d_k$ . Let  $f$  be defined as  $f(x) = \beta^{-1}(1 - e^{-\beta x})$ . Define the domain of the total outcome  $\mathcal{I} = [C_0 + G_{\min}, C_0 + G_{\max}]$ , which leads to the effective risk aversion coefficient  $\beta$  on this domain

$$\beta = \frac{\inf_{z \in \mathcal{I}} f''(z)}{\inf_{z \in \mathcal{I}} f'(z)}.$$

Then, using the range of the returns  $\Delta_G = G_{\max} - G_{\min}$ , the value function satisfies

$$V_t(s, c) \geq \mathbb{E}[G_t(s, c)] - \frac{d_t}{8} \beta \Delta_G^2.$$

*Proof.* Let  $X = d_t c + d_t G_t(s, c)$  be the random variable representing the total accumulated value. Let  $\mu_X = \mathbb{E}[X]$  and  $\sigma_X^2 = \mathbb{E}[(X - \mu_X)^2] = \text{Var}(X)$ . We divide this proof in three main steps:

**Step 1 – Bounding the Expected Utility.** We use Taylor's theorem with the Lagrange remainder form. For any realization  $x \in \mathcal{I}$ , expanding  $f(x)$  around the mean  $\mu_X$  gives

$$f(x) = f(\mu_X) + f'(\mu_X)(x - \mu_X) + \frac{1}{2} f''(\xi_x)(x - \mu_X)^2,$$

where  $\xi_x \in (x, \mu_X)$ . Since  $f$  is concave,  $f''(z) \leq 0$ . We define  $M_{f''} = \inf_{z \in \mathcal{I}} f''(z)$ , a negative value representing the maximum magnitude of the second derivative (i.e., highest curvature). We have  $f''(\xi_x) \geq M_{f''}$  and thus

$$f(x) \geq f(\mu_X) + f'(\mu_X)(x - \mu_X) + \frac{1}{2} M_{f''}(x - \mu_X)^2.$$

Taking the expectation leads to

$$\mathbb{E}[f(X)] \geq f(\mu_X) + \frac{1}{2} M_{f''} \sigma_X^2. \quad (15)$$

**Step 2 – Applying the Inverse Function.** Let  $y_0 = f(\mu_X)$  and  $\Delta = \frac{1}{2} M_{f''} \sigma_X^2$ . Applying the strictly increasing function  $f^{-1}$  to (15) and performing a Taylor expansion of  $f^{-1}(y_0 + \Delta)$  around  $y_0$ , we obtain the following inequality for the certainty equivalent  $\text{CE}_f(X) = f^{-1}(\mathbb{E}[f(X)])$ :

$$\text{CE}_f(X) \geq f^{-1}(y_0 + \Delta) = f^{-1}(y_0) + (f^{-1})'(\zeta) \cdot \Delta,$$

where  $\zeta \in (y_0 + \Delta, y_0)$ . The derivative of the inverse function is  $(f^{-1})'(y) = \frac{1}{f'(f^{-1}(y))}$ . Denoting  $z = f^{-1}(\zeta)$ , we have

$$\text{CE}_f(X) \geq \mu_X + \frac{1}{f'(z)} \Delta. \quad (16)$$

To maintain the direction of the inequality, we must bound the term  $\frac{1}{f'(z)} \Delta$  from below. Since  $\Delta$  is negative by concavity of  $f$ , this requires finding an *upper* bound for the positive multiplier  $\frac{1}{f'(z)}$ . An upper bound on the reciprocal requires a *lower* bound on the denominator. Let  $m_{f'} = \inf_{z \in \mathcal{I}} f'(z)$ . Assuming  $f$  is strictly increasing,  $m_{f'} > 0$ . Then  $f'(z) \geq m_{f'}$  implies  $\frac{1}{f'(z)} \leq \frac{1}{m_{f'}}$ . Multiplying the inequality  $\frac{1}{f'(z)} \leq \frac{1}{m_{f'}}$  by the negative number  $\Delta$  reverses the inequality to  $\frac{\Delta}{f'(z)} \geq \frac{\Delta}{m_{f'}}$ . Substituting this back into (16) and using the definition  $\beta = |M_{f''}|/m_{f'}$ , we get

$$\text{CE}_f(X) \geq \mu_X + \frac{1}{m_{f'}} \left( \frac{1}{2} M_{f''} \sigma_X^2 \right) = \mu_X - \frac{1}{2} \beta \sigma_X^2.$$

**Step 3 – Bounding the Value Function.** Finally, we can substitute  $\text{CE}_f$  into the definition of  $V_t(s, c)$  to bound the value function:

$$\begin{aligned} V_t(s, c) &\stackrel{(a)}{\geq} \frac{(\mu_X - \frac{1}{2} \beta \sigma_X^2) - d_t c}{d_t} \\ &\stackrel{(b)}{\geq} \mathbb{E}[G_t(s, c)] - \frac{d_t}{2} \beta \text{Var}(G_t(s, c)) \\ &\stackrel{(c)}{\geq} \mathbb{E}[G_t(s, c)] - \frac{d_t}{8} \beta \Delta_G^2. \end{aligned}$$

**(a)** follows from applying the previous inequality on  $V_t(s, c) = \frac{1}{d_t}(\text{CE}_f(X) - d_t c)$ . **(b)** comes from  $\mu_X = d_t c + d_t \mathbb{E}[G_t(s, c)]$  and  $\sigma_X^2 = d_t^2 \text{Var}(G_t(s, c))$ . **(c)** is true by Popoviciu's inequality  $\text{Var}(G_t) \leq \frac{\Delta_G^2}{4}$ .  $\square$

Using this lemma, we can derive a performance bound for the infinite-horizon optimal policy using the approximation scheme described in Algorithm 1. The following proof provides a bound for the performance of the policy returned by Algorithm 1 for any stock  $c \in \mathcal{C}$ , corresponding to the DP errors of the inner optimization. To relate this bound to the OCE risk measure, one must perform the outer optimization via a grid search and approximately solve the OCE, in a similar manner to Steps 2 and 3 of the proof of Proposition 3.5. The performance analysis then depends on both the grid range and its level of discretization.

**Theorem F.3** (Performance Bound for Approximate Infinite-Horizon Policy (Restated)). *Let the objective functional  $K$  be the Entropic Risk Measure with risk aversion coefficient  $\beta > 0$  (corresponding to the exponential utility  $f(x) = \beta^{-1}(1 - e^{-\beta x})$ ). Let the discount function  $d_t$  follow the truncation scheme with parameter  $\gamma_{tail} < 1$  for  $t \geq T'$ . Let  $\pi^*$  be the optimal non-stationary policy for the infinite-horizon problem,  $\hat{\pi}^*$  the policy returned by Algorithm 1 with planning horizon  $T'$ , and  $\Delta_G$  the range of the discounted returns. Then, the suboptimality of the approximate policy at time  $t = 0$  is bounded by*

$$\|F_K(\eta_0^{\pi^*}) - F_K(\eta_0^{\hat{\pi}^*})\|_\infty \leq \frac{d_{T'}^2 \cdot \beta \cdot \Delta_G^2}{8}.$$

### Proof of Theorem 5.2. Step 1 – Bounding the Error at the Truncation Horizon

We first establish a bound on the difference between the risk-neutral value and the CE value for any policy  $\pi$ . Let  $V_t^{\pi, \text{RN}}(s, c) \doteq \mathbb{E}[G_t^\pi(s, c)]$  denote the discounted risk-neutral value function (i.e., expected return), and let  $V_t^{\pi, \text{CE}}(s, c)$  denote the discounted CE value function. Using the lower bound for the certainty equivalent value function from Lemma F.2, for any policy  $\pi$ , time  $t$ , state  $s \in \mathcal{S}$ , and stock  $c \in \mathcal{C}$ , we have  $V_t^{\pi, \text{CE}}(s, c) \geq V_t^{\pi, \text{RN}}(s, c) - \mathcal{E}_t$ , where we denote  $\mathcal{E}_t = \frac{d_t}{8} \beta \Delta_G^2$ . Conversely, by the concavity of the utility function  $f$  [Proposition 2.2 in Ben-Tal & Teboulle, 2007], the CE is upper-bounded by the expectation. Thus,

$$0 \stackrel{(a)}{\leq} V_t^{\pi, \text{RN}}(s, c) - V_t^{\pi, \text{CE}}(s, c) \stackrel{(b)}{\leq} \mathcal{E}_t, \quad (17)$$

where **(a)** holds because  $\mathbb{E}$  is an upper-bound on the CE, and **(b)** follows from Lemma F.2.

We now bound the difference between the optimal value function of the infinite-horizon discounted CE-MDP,  $V_{T'}^{\pi^*, \text{CE}}$ , and the value function returned by Algorithm 1,  $V_{T'}^{\hat{\pi}^*, \text{CE}}$ , at the planning horizon  $T'$  and for any state and stock  $(s, c)$  as follows:

$$\begin{aligned} V_{T'}^{\pi^*, \text{CE}}(s, c) - V_{T'}^{\hat{\pi}^*, \text{CE}}(s, c) &\stackrel{(a)}{\leq} V_{T'}^{\pi^*, \text{CE}}(s, c) - V_{T'}^{\hat{\pi}^*, \text{RN}}(s, c) + \mathcal{E}_{T'} \\ &\stackrel{(b)}{\leq} V_{T'}^{\pi^*, \text{RN}}(s, c) - V_{T'}^{\hat{\pi}^*, \text{RN}}(s, c) + \mathcal{E}_{T'} \\ &\stackrel{(c)}{\leq} \mathcal{E}_{T'}. \end{aligned}$$

Here, **(a)** follows from the RHS of (17) for  $\hat{\pi}^*$ . **(b)** comes from the fact that using the LHS of (17) for the optimal CE policy  $\pi^*$ , we have  $0 \leq V_{T'}^{\pi^*, \text{RN}} - V_{T'}^{\pi^*, \text{CE}} \implies V_{T'}^{\pi^*, \text{CE}} \leq V_{T'}^{\pi^*, \text{RN}}$ . **(c)** is true because  $\hat{\pi}_{T'}^* = \pi_{\text{RN}}^* \in \arg \max_\pi V_{T'}^{\pi, \text{RN}}$  is the policy that maximizes the expected return. Thus,  $V_{T'}^{\pi^*, \text{RN}}(s, c) \leq V_{T'}^{\hat{\pi}^*, \text{RN}}(s, c)$ , making the difference non-positive for all  $(s, c) \in \mathcal{S} \times \mathcal{C}$ .

### Step 2 – Constructing a Lower Bound for the Value of the Approximate Policy

We construct a value function  $U_t$  and a corresponding return distribution function  $\eta_t^{\text{LB}}$  for all  $t \in 0 : T'$  which serves as a lower bound for the true CE value of the algorithm's policy  $V_t^{\hat{\pi}^*, \text{CE}}$ . This construction proceeds by backward induction.

**Base Case ( $t = T'$ ):** The algorithm defines the policy  $\hat{\pi}^*$  such that for  $t \geq T'$ ,  $\hat{\pi}_t^* = \pi_{\text{RN}}^*$ . Therefore, the true CE value of the algorithm's policy at the horizon is the CE value of the risk-neutral policy. In addition, the algorithm initializes its computation with the risk-neutral value:  $\hat{V}_{T'}^*(s, c) = V_{T'}^{\pi_{\text{RN}}^*, \text{RN}}(s, c)$ . Using the bound established in (17) of Step 1 applied to the policy  $\pi = \pi_{\text{RN}}^*$ , we have:

$$V_{T'}^{\hat{\pi}^*, \text{CE}}(s, c) = V_{T'}^{\pi_{\text{RN}}^*, \text{CE}}(s, c) \geq V_{T'}^{\pi_{\text{RN}}^*, \text{RN}}(s, c) - \mathcal{E}_{T'}.$$

We define the lower-bound return distribution  $\eta_{T'}^{\text{LB}}$  by shifting the algorithm's terminal distribution by the constant error  $\mathcal{E}_{T'}$ :

$$\eta_{T'}^{\text{LB}}(s, c) \doteq \text{shift}(\hat{\eta}_{T'}^*(s, c), -\mathcal{E}_{T'}).$$

Let  $U_{T'}(s, c) = F_K(\eta_{T'}^{\text{LB}})(s, c)$ . By the translation invariance of  $F_K$ , we have

$$U_{T'}(s, c) = F_K(\hat{\eta}_{T'}^*)(s, c) - \mathcal{E}_{T'} = \hat{V}_{T'}^*(s, c) - \mathcal{E}_{T'}.$$

Combining these yields the base case inequality

$$V_{T'}^{\hat{\pi}^*, \text{CE}}(s, c) \geq U_{T'}(s, c).$$

**Recursive Step** ( $t < T'$ ): We define  $U_t$  and the corresponding  $\eta_t^{\text{LB}}$  recursively using the Bellman operator for the algorithm's policy  $\hat{\pi}_t^*$ :

$$U_t = F_K \eta_t^{\text{LB}} \quad \text{and} \quad \eta_t^{\text{LB}} = \mathcal{T}_{\hat{\pi}_t^*}^d \eta_{t+1}^{\text{LB}}.$$

Assume that for some  $t+1 \leq T'$ , the hypothesis  $V_{t+1}^{\hat{\pi}^*, \text{CE}}(s, c) \geq U_{t+1}(s, c)$  holds. We aim to show that  $V_t^{\hat{\pi}^*, \text{CE}}(s, c) \geq U_t(s, c)$  is true at time  $t$ . By definition,  $V_{t+1}^{\hat{\pi}^*, \text{CE}} = F_K \eta_{t+1}^{\hat{\pi}^*}$  and  $U_{t+1} = F_K \eta_{t+1}^{\text{LB}}$ . Thus, the hypothesis implies

$$F_K \eta_{t+1}^{\hat{\pi}^*} \geq F_K \eta_{t+1}^{\text{LB}}.$$

We now apply the Time-Dependent Monotonicity from Lemma 3.1. Since the objective functional is monotonic, applying the Bellman operator for the fixed policy  $\hat{\pi}_t^*$  preserves the preference order:

$$F_K(\mathcal{T}_{\hat{\pi}_t^*}^d \eta_{t+1}^{\hat{\pi}^*}) \geq F_K(\mathcal{T}_{\hat{\pi}_t^*}^d \eta_{t+1}^{\text{LB}}).$$

The LHS is the definition of the true value  $V_t^{\hat{\pi}^*, \text{CE}}(s, c)$ , while the RHS is the definition of  $U_t(s, c)$ . Therefore, we recover the desired inequality

$$V_t^{\hat{\pi}^*, \text{CE}}(s, c) \geq U_t(s, c).$$

**Relationship between  $\hat{\pi}^*$  and  $U$ :** Finally, we characterize the difference between the algorithm's value function  $\hat{V}_t^*$  and the lower bound  $U_t$ . By construction,  $\eta_{T'}^{\text{LB}}$  differs from  $\hat{\eta}_{T'}^*$  by a constant shift of  $-\mathcal{E}_{T'}$ . Due to the structure of the Time-Dependent Bellman operator, where the future outcome is scaled by the one-step discount factor  $\hat{d}_t$ , a constant shift of  $\Delta$  at time  $t+1$  propagates as a shift of  $\hat{d}_t \Delta$  at time  $t$ . Since  $\hat{\pi}_t^*$  is used for both transitions, and  $F_K$  is translation invariant, the error propagates deterministically backwards:

$$U_t(s, c) = \hat{V}_t^*(s, c) - \left( \prod_{k=t}^{T'-1} \hat{d}_k \right) \mathcal{E}_{T'}.$$

The term being subtracted depends only on  $t$  and  $T'$ , not on the state  $s$  or stock  $c$ . Since the greedy operator  $\text{argmax}_{\pi} F_K \mathcal{T}_{\pi}^d V$  is invariant to adding a constant to the value function  $V$ , the policy  $\hat{\pi}_t^*$  computed by the algorithm (which is greedy with respect to  $\hat{V}_{t+1}^*$ ) is also greedy with respect to  $U_{t+1}$ .

### Step 3 – Bounding the Distance to the True Optimal Value

We aim to show that for each state  $s$ , stock  $c$ , and time  $t \in 0 : T'$ , the difference between the true optimal value and the lower bound constructed in Step 2 satisfies

$$V_t^{*, \text{CE}}(s, c) - U_t(s, c) \leq \delta_t. \quad (18)$$

where we define the sequence of bounds  $\delta_t$  as

$$\delta_t \doteq \left( \prod_{k=t}^{T'-1} \hat{d}_k \right) \mathcal{E}_{T'}.$$

Note that this sequence satisfies the recurrence relation  $\delta_t = \hat{d}_t \delta_{t+1}$  for  $t < T'$ , and  $\delta_{T'} = \mathcal{E}_{T'}$ . Also, note that  $\prod_{k=t}^{T'-1} \hat{d}_k = \frac{d_{T'}}{d_t}$ . We prove (18) by backward induction.

**Base Case:** The inequality holds trivially for  $t = T'$ , because the risk-averse optimal value is upper-bounded by the risk-neutral optimal value, i.e.,  $V_{T'}^{*, \text{CE}} \leq V_{T'}^{*, \text{RN}} = V_{T'}^{\pi_{\text{RN}}^*, \text{RN}}$ , and thus:

$$\begin{aligned} V_{T'}^{*, \text{CE}}(s, c) - U_{T'}(s, c) &= V_{T'}^{*, \text{CE}}(s, c) - \left( \hat{V}_{T'}^*(s, c) - \mathcal{E}_{T'} \right) \\ &= V_{T'}^{*, \text{CE}}(s, c) - V_{T'}^{\pi_{\text{RN}}^*, \text{RN}}(s, c) + \mathcal{E}_{T'} \\ &\leq V_{T'}^{\pi_{\text{RN}}^*, \text{RN}}(s, c) - V_{T'}^{\pi_{\text{RN}}^*, \text{RN}}(s, c) + \mathcal{E}_{T'} \\ &= \mathcal{E}_{T'}. \end{aligned}$$

**Recursive Step:** Assuming that the hypothesis (18) holds for  $t + 1$  for each  $(s, c) \in \mathcal{S} \times \mathcal{C}$ , we show that, for  $t$  and all  $(s, c)$ , we obtain the following:

$$\begin{aligned}
 V_t^{*,\text{CE}}(s, c) - U_t(s, c) &\stackrel{(a)}{=} (F_K \mathcal{T}_{\pi_t^*}^d \eta_{t+1}^*)(s, c) - (F_K \mathcal{T}_{\hat{\pi}_t^*}^d \eta_{t+1}^{\text{LB}})(s, c) \\
 &\stackrel{(b)}{\leq} (F_K \mathcal{T}_{\pi_t^*}^d \eta_{t+1}^*)(s, c) - (F_K \mathcal{T}_{\pi_t^*}^d \eta_{t+1}^{\text{LB}})(s, c) \\
 &\stackrel{(c)}{=} \frac{1}{d_t} \left( \text{CE}_f(d_{t+1} V_{t+1}^{*,\text{CE}}(S', C')) - \text{CE}_f(d_{t+1} U_{t+1}(S', C')) \right) \\
 &\stackrel{(d)}{\leq} \frac{1}{d_t} (\text{CE}_f(d_{t+1}(U_{t+1}(S', C') + \delta_{t+1})) - \text{CE}_f(d_{t+1} U_{t+1}(S', C'))) \\
 &\stackrel{(e)}{=} \frac{1}{d_t} (d_{t+1} \delta_{t+1} + \text{CE}_f(d_{t+1} U_{t+1}(S', C')) - \text{CE}_f(d_{t+1} U_{t+1}(S', C'))) \\
 &= \hat{d}_t \cdot \delta_{t+1} = \delta_t.
 \end{aligned}$$

(a) holds by the definition of  $V^*$  and  $U$ . (b) follows because  $\hat{\pi}_t^*$  is greedy with respect to  $U_{t+1}$  (from Step 2), so replacing it with  $\pi_t^*$  in the second term can only decrease the value. (c) utilizes the recursive definition of the value function derived from the Bellman operator, where the value at  $t + 1$  acts as the random variable for the CE at  $t$ .  $S'$  and  $C'$  denote the random next state and stock. (d) uses the monotonicity of  $\text{CE}_f$  and the inductive hypothesis  $V_{t+1}^* \leq U_{t+1} + \delta_{t+1}$ . (e) follows from the translation invariance property of the CE functional  $\text{CE}_f(X + k) = \text{CE}_f(X) + k$ . Here, the constant shift is  $d_{t+1} \delta_{t+1}$ .

Unrolling the recursion to  $t = 0$ , and noting that  $U_0(s_0, c_0) \leq V_0^{\hat{\pi}^*,\text{CE}}(s_0, c_0)$  from Step 2, we obtain the final bound

$$\|V_0^{*,\text{CE}} - V_0^{\hat{\pi}^*,\text{CE}}\|_\infty \leq d_{T'} \mathcal{E}_{T'} = \frac{d_{T'}^2 \cdot \beta \cdot \Delta_G^2}{8}.$$

This completes the proof, showing that the performance loss is  $\mathcal{O}(d_{T'}^2)$ .  $\square$

**Lemma F.4** (Lower Bound for Mean-CVaR Value Function). *Let the utility function be defined as the Mean-CVaR utility*

$$f(x) = \kappa_1(x)_+ + \kappa_2(x)_-,$$

where  $\kappa_2 > \kappa_1 > 0$ . Let the value function at time  $t$  for a state  $s \in \mathcal{S}$  and scaled stock  $c \in \mathcal{C}$  be defined as

$$V_t(s, c) \doteq \frac{1}{d_t} (f^{-1}(\mathbb{E}[f(d_t c + d_t G_t(s, c))]) - d_t c),$$

where  $d_t > 0$  is the discount factor and  $G_t(s, c)$  is the random future return. Let  $\Lambda = \frac{\kappa_2 - \kappa_1}{\kappa_1} > 0$  be the coefficient of loss aversion. Then, the value function is bounded from below by the expected return minus a first-order risk penalty:

$$V_t(s, c) \geq \mathbb{E}[G_t(s, c)] - \Lambda \mathbb{E}[|(c + G_t(s, c))_-|].$$

*Proof.* Let  $X = d_t c + d_t G_t(s, c)$  be the random variable representing the total accumulated value. As opposed to the proof of Lemma F.2, we directly bound the inverse function:

**Step 1 – Representing the Utility.** The piecewise linear utility function can be rewritten as a linear term plus a penalty for negative outcomes, that is  $f(x) = \kappa_1 x + (\kappa_2 - \kappa_1)(x)_-$ , where  $(x)_- = \min(0, x)$ . Note that since  $\kappa_2 > \kappa_1 > 0$ , the coefficient  $(\kappa_2 - \kappa_1)$  is positive, and  $f$  is both strictly increasing and concave. Taking the expectation yields

$$\mathbb{E}[f(X)] = \kappa_1 \mathbb{E}[X] + (\kappa_2 - \kappa_1) \mathbb{E}[(X)_-].$$

**Step 2 – Bounding the Inverse Function.** For any utility function  $f$  that is strictly increasing, concave, and for which its inverse  $f^{-1}$  is bounded from below by some function  $g$ , we have that

$$V_t(s, c) \geq \frac{1}{d_t} (g(\mathbb{E}[f(X)]) - d_t c).$$

We seek to bound  $f^{-1}(y)$ . Since  $f(0) = 0$ , the inverse function is given by

$$f^{-1}(y) = \begin{cases} \frac{y}{\kappa_1} & \text{if } y \geq 0 \\ \frac{y}{\kappa_2} & \text{if } y < 0 \end{cases}$$

Since  $\kappa_1 < \kappa_2$  and we are dividing a negative number in the  $y < 0$  case, dividing by the larger  $\kappa_2$  yields a value closer to 0 (i.e., larger) than dividing by  $\kappa_1$ . Thus, for all  $y \in \mathbb{R}$ ,

$$f^{-1}(y) \geq \frac{y}{\kappa_1}.$$

**Step 3 – Bounding the Value Function.** We substitute the expression from Step 1 into the bound of  $V_t(s, c)$  from Step 2:

$$V_t(s, c) \geq \frac{\mathbb{E}[X] + \Lambda \mathbb{E}[(X)_-] - d_t c}{d_t},$$

where  $\Lambda = \frac{\kappa_2 - \kappa_1}{\kappa_1}$ . Using  $X = d_t c + d_t G_t$ , we have that  $\mathbb{E}[X] = d_t c + d_t \mathbb{E}[G_t]$ . Also, since  $d_t > 0$ , we have  $(d_t(c + G_t))_- = d_t(c + G_t)_-$ . Finally,  $(z)_- = -|z|$  by definition. Altogether, we obtain the final bound on the value function

$$\begin{aligned} V_t(s, c) &\geq \frac{(d_t c + d_t \mathbb{E}[G_t]) + \Lambda d_t \mathbb{E}[(c + G_t)_-] - d_t c}{d_t} \\ &= \mathbb{E}[G_t] + \Lambda \mathbb{E}[(c + G_t)_-] \\ &= \mathbb{E}[G_t] - \Lambda \mathbb{E}[|(c + G_t)_-|]. \end{aligned}$$

□

**Remark F.5** (Asymptotic Risk-Neutrality via Stock Growth). Unlike the differentiable case, the risk penalty  $\Lambda \mathbb{E}[|(c_t + G_t)_-|]$  does not explicitly scale with  $d_t$ . However, asymptotic convergence to risk-neutrality is driven by the stock dynamics. Recall that  $c_t = d_t^{-1} (C_0 + \sum_{k=0}^{t-1} d_k R_{k+1})$ . Assuming positive rewards, the accumulated sum in the numerator is positive and non-decreasing. As  $d_t \rightarrow 0$ , the factor  $d_t^{-1}$  drives  $c_t \rightarrow +\infty$ . Because the future return  $G_t$  is uniformly bounded, there exists a time  $t$  after which the accumulated stock  $c_t$  is large enough to absorb any possible future negative fluctuation. Consequently, the shortfall term  $(c_t + G_t)_-$  becomes identically zero, and the value function converges exactly to the expected return  $\mathbb{E}[G_t]$ .

**Remark F.6** (Asymptotic Indifference of Pure CVaR). The convergence to risk-neutrality discussed in Lemma 8 and Remark 13 relies on the utility function being strictly increasing (e.g., Mean-CVaR with  $\kappa_1 > 0$ ). In the specific case of Pure CVaR ( $\kappa_1 = 0$ ), the utility function  $f(x) = \frac{1}{\alpha}(x)_-$  becomes constant for all  $x \geq 0$ . As  $d_t \rightarrow 0$  implies  $c_t \rightarrow \infty$  (under positive rewards), the risk penalty term eventually vanishes, but there is no remaining linear term to drive the maximization of the expected return. Consequently, the agent does not converge to a risk-neutral policy, but rather to an *indifferent* policy: once the accumulated stock is sufficient to ensure safety, the objective function saturates at zero, the gradients vanish, and any action that maintains this safety level is considered optimal. In practice, using Mean-CVaR with a small  $\kappa_1 > 0$  is essential to maintain a valid learning signal in this asymptotic regime.

**Corollary F.7** (Performance Bound for Mean-CVaR Value Function). *Let the utility function be defined as the Mean-CVaR utility*

$$f(x) = \kappa_1(x)_+ + \kappa_2(x)_-,$$

where  $\kappa_2 > \kappa_1 > 0$ . This ensures  $f$  is strictly increasing and concave. Let the value function at time  $t$  for a state  $s \in \mathcal{S}$  and scaled stock  $c \in \mathcal{C}$  be defined as

$$V_t(s, c) \doteq \frac{1}{d_t} (f^{-1}(\mathbb{E}[f(d_t c + d_t G_t(s, c))]) - d_t c),$$

where  $d_t > 0$  is the discount factor and  $G_t(s, c)$  is the random future return. Let the discount function  $d_t$  follow the truncation scheme with parameter  $\gamma_{\text{tail}} < 1$  for  $t \geq T'$ . Let  $\pi^*$  be the optimal non-stationary policy for the infinite-horizon problem,  $\hat{\pi}^*$  the policy returned by Algorithm 1 with planning horizon  $T'$ , and  $\Lambda = \frac{\kappa_2 - \kappa_1}{\kappa_1} > 0$  be the coefficient of loss aversion. Then, the suboptimality of the approximate policy at time  $t = 0$  is bounded by

$$\|F_K(\eta_0^{\pi^*}) - F_K(\eta_0^{\hat{\pi}^*})\|_\infty \leq d_{T'} \Lambda \mathbb{E}[|(c + G_t(s, c))_-|].$$

*Proof.* The proof follows step-by-step the derivations in the theorem below, where we replace  $\mathcal{E}_t$  with the lower bound for the mean-CVaR value function

$$\mathcal{E}_t = \Lambda \mathbb{E}[|(c + G_t(s, c))_-|].$$

It leads in a straightforward way to

$$\|V_0^{*,\text{CE}} - V_0^{\hat{\pi}^*,\text{CE}}\|_\infty \leq d_{T'} \mathcal{E}_{T'} = d_{T'} \Lambda \mathbb{E}[|(c + G_t(s, c))_-|]$$

□

## G The RIGOR Algorithm

Our algorithm for **R**Isk-sensitive RL under **G**eneral discounting **O**f **R**eturns (RIGOR) is based on the principles of QR-DQN [Dabney et al., 2018] and D $\eta$ N [Pires et al., 2025]. It learns return distributions under general discount functions and optimizes a risk-adjusted return using an OCE risk measure. The core of the RIGOR agent is a neural network, parameterized by  $\theta$ , that approximates the marginal return distribution. The network takes the augmented state  $(s_t, t, c_{d,t})$  as input and outputs a set of quantile predictions for each action.

For state  $(s_t, t, c_{d,t})$ , the agent queries the network to get the predicted quantile function, denoted by  $\{\xi_\theta(\cdot | s_t, t, c_{d,t}, a)\}_j$ . Specifically,  $\xi_\theta$  returns the quantile function evaluated at the points  $\{\tau_j\}_{j=1}^n$ . Using these quantiles as an empirical representation of the distribution, the agent evaluates the expected utility of the total outcome. This is estimated by averaging the utility function  $f$  over the reconstructed samples of the total return:

$$Q(s_t, t, c_{d,t}, a) \approx \frac{1}{n} \sum_{j=1}^n f(d_t c_{d,t} + d_t \xi_\theta(s_t, t, c_{d,t}, a)_j) / d_t.$$

If the utility function  $f$  is invariant to scaling, this can be written as

$$Q(s_t, t, c_{d,t}, a) \approx \frac{1}{n} \sum_{j=1}^n f(c_{d,t} + \xi_\theta(s_t, t, c_{d,t}, a)_j).$$

The agent selects the action  $a_t^*$  that maximizes this estimated expected utility. To ensure the predictions are accurate, the network is trained using the quantile regression loss with a target network  $\bar{\theta}$  to generate stable temporal difference targets. We include a replay buffer and employ mini-batching when computing the loss function:

$$\frac{1}{B} \sum_{k=1}^B \sum_{j=1}^n \sum_{l=1}^n \ell(y_j^k - \xi_\theta(s^k, t^k, c_d^k, a^k)_l, \tau_l), \quad (19)$$

where the target is  $y_j^k = r^k + \hat{d}_t \xi_{\bar{\theta}}(s'^k, t'^k, c'_d, a'^k)_j$ . The function  $\ell(u, \tau) = u(\tau - \mathbb{I}_{u < 0})$  is the standard quantile regression loss (tilted absolute value). We provide an outline of this approach in Algorithm 2.

The range for the initial stock is chosen to correspond to the negative of the potential discounted return range of the environment. Both the discretization granularity and the frequency of the outer optimization loop can be tuned for each specific environment. For instance, in the risk-sensitive optimization for the Goal-Based Wealth Management (GBWM) environment, where returns can reach up to 4000, we set the initial stock range to  $[-4000, 0]$  and discretize it into 201 equal intervals. Additionally, in this experiment, the initial stock is updated after every 1000 value function updates.

**Multi-Horizon RIGOR Algorithm.** To approximate the marginal return distributions for a fixed set of discount factors  $\Gamma = \{\gamma_i\}_{i=1}^m$ , we extend the architecture to output a set of quantile predictions for each of the  $m$  return streams. The utility estimation is further adapted to account for the weighted sum of these streams:

$$Q(s_t, t, c_{d,t}, a) \approx \frac{1}{n} \sum_{j=1}^n f \left( \tilde{d}_t c_{d,t} + \sum_{i=1}^m w_i \gamma_i^t \xi_\theta(s_t, t, c_{d,t}, a)_{i,j} \right) / \tilde{d}_t,$$

where  $w_{i,t} = \frac{w_i \gamma_i^t}{\sum_{j=1}^m w_j \gamma_j^t}$ . The network is trained by applying the quantile regression loss independently to each of the  $m$  return streams. The full loss function becomes

$$\frac{1}{B} \sum_{k=1}^B \left( \sum_{i=1}^m \frac{1}{n^2} \sum_{j=1}^n \sum_{l=1}^n \ell \left( y_{i,j}^k - \xi_\theta(s^k, t^k, c_d^k, a^k)_{i,l}, \tau_l \right) \right), \quad (20)$$

where the target for each horizon is  $y_{i,j}^k = r^k + \gamma_i \xi_{\bar{\theta}}(s'^k, t'^k, c'_d, a'^k)_{i,j}$ . We provide an outline of the multi-horizon algorithm in Algorithm 3. For both RIGOR algorithms, the choice of hyperparameters is application-dependent and described in Appendix H.

## H Additional Details of the Experimental Results

We implement our algorithm based on the single-file RL implementations from CleanRL [Huang et al., 2022], where the model and its training loop are encapsulated within a single script. For option trading, windy lunar lander, and GBWM experiments, we use a feed-forward neural network of 2 hidden layers, with 120 and 84 neurons, respectively. The network parameters are updated using the Adam optimizer with a learning rate of 0.001. We set the number of quantiles to  $n = 200$ , the Huber loss to  $\tau = 0.1$ , the target smoothing coefficient to  $\alpha = 0.005$ , and the mini-batch sizes to 256.

**Algorithm 2** RIGOR Algorithm

---

**Input:** Quantiles  $\{\tau_j\}_{j=1}^n$ , Learning rate  $\lambda$ , Target smoothing coefficient  $\alpha$ , Batch size  $B$ , Discount function  $d(\cdot)$ , Utility function  $f$ , Discretized Range for Initial Stock  $\bar{\mathcal{C}}$   
 Initialize network  $\theta$ , target network  $\bar{\theta} \leftarrow \theta$ , replay buffer  $\mathcal{D}$   
 Define  $Q(s, t, c, a; \theta) := \frac{1}{n} \sum_{j=1}^n f(d_t c + d_t \xi_\theta(s, t, c, a)_j) / d_t$   
**for** each outer optimization update **do**  
**for** each  $c_{d,0} \in \bar{\mathcal{C}}$  **do**  
 Set  $a_0(c_{d,0}) \leftarrow \arg \max_{a \in \mathcal{A}} Q(s_0, 0, c_{d,0}, a; \theta)$   
**end for**  
 Set the initial stock  $c_{d,0} \leftarrow \arg \max_{c \in \bar{\mathcal{C}}} \{-c + Q(s_0, 0, c, a_0(c); \theta)\}$   
**for** each environment step **do**  
 Observe state  $(s_t, t, c_{d,t})$   
 Select  $a_t \sim \epsilon\text{-greedy}(\arg \max_{a \in \mathcal{A}} Q(s_t, t, c_{d,t}, a; \theta))$   
 Execute  $a_t$ , observe  $r_{t+1}, s_{t+1}$   
 Compute the stock  $c_{d,t+1} \leftarrow (c_{d,t} + r_{t+1}) / \hat{d}_t$   
 Store  $(s_t, t, c_{d,t}, a_t, r_{t+1}, s_{t+1}, t+1, c_{d,t+1})$  in  $\mathcal{D}$   
**if** update is scheduled **then**  
 Sample batch  $\{(s^k, t^k, c_d^k, a^k, r^k, s'^k, t'^k, c_d'^k)\}_{k=1}^B$  from  $\mathcal{D}$   
**for** each sample  $k$  **do**  
 Compute  $a'^k \leftarrow \arg \max_{a \in \mathcal{A}} Q(s'^k, t'^k, c_d'^k, a; \theta)$   
 Compute  $y_j^k \leftarrow r^k + \hat{d}_{t^k} \xi_{\bar{\theta}}(s'^k, t'^k, c_d'^k, a'^k)_j$  for  $j = 1, \dots, n$   
**end for**  
 Compute loss  $L_\theta$  using Eq. (19)  
 Update network:  $\theta \leftarrow \theta - \lambda_\theta \nabla_\theta L$   
 Update target network:  $\bar{\theta} \leftarrow (1 - \alpha) \bar{\theta} + \alpha \theta$   
**end if**  
**end for**  
**end for**

---

## H.1 American Put Option Trading

In this environment, the underlying asset price is modeled as an Ornstein–Uhlenbeck process, evolving according to

$$dP_t = \kappa(\zeta - P_t) dt + \sigma dW_t,$$

where  $\zeta = 100$  denotes the long-term mean level,  $\kappa = 2$  controls the rate at which the process reverts toward the mean,  $\sigma = 20$  is the volatility parameter, and  $W_t$  is a standard Brownian motion. The initial price is set to  $P_0 = 100$ , and the strike price of the put option is fixed at  $K = 100$ . At each time step, the agent may either exercise the option to obtain an immediate payoff  $r_t = \max\{0, K - P_t\}$  or continue holding the option in anticipation of a future reward. If the option is not exercised prior to maturity, the terminal payoff is automatically realized as  $r_T = \max\{0, K - P_T\}$ .

## H.2 Windy Lunar Lander

The Lunar Lander task is a benchmark control problem focused on optimizing the descent and landing of a rocket under physics-based dynamics. The environment is described by an 8-dimensional continuous state representation, and the agent can choose among four discrete actions: activating the left or right attitude thrusters, engaging the main engine, or taking no action. To make the dynamics non-deterministic, the wind disturbance is enabled. The goal is to steer the lander from an initial position near the top of the screen to the designated landing zone. A successful touchdown typically results in a cumulative reward between 100 and 140. Deviations that carry the lander away from the landing pad are penalized, while a crash incurs an additional reward of  $-100$ . A safe landing grants a bonus of  $+100$ , and each landing leg that touches the ground contributes an extra  $+10$ . Engine usage is discouraged through fuel costs: firing the main engine yields a penalty of  $-0.3$  per time step, and using either side engine results in a penalty of  $-0.03$  per time step.

## H.3 Goal-Based Wealth Management

Regarding the available portfolios, we follow the framework from Das et al. [2022], who used portfolios on the efficient frontier generated by index funds representing U.S. Bonds, International Stocks, and U.S. Stocks over a 20-year period

---

**Algorithm 3** Multi-Horizon RIGOR Algorithm

---

**Input:** Quantiles  $\{\tau_j\}_{j=1}^n$ , Learning rate  $\lambda$ , Target smoothing coefficient  $\alpha$ , Batch size  $B$ , Discount factors  $\Gamma = \{\gamma_i\}_{i=1}^m$ , Fixed weights  $\mathbf{w}$ , Utility function  $f$ , Discretized Range for Initial Stock  $\bar{\mathcal{C}}$   
 Initialize network  $\theta$ , target network  $\bar{\theta} \leftarrow \theta$ , replay buffer  $\mathcal{D}$   
 Define  $\tilde{d}_t := \sum_{j=1}^m w_j \gamma_j^t$   
 Define  $Q(s, t, c, a; \theta) := \frac{1}{n} \sum_{j=1}^n f \left( \tilde{d}_t c + \sum_{i=1}^m w_i \gamma_i^t \xi_\theta(s, t, c, a)_{i,j} \right) / \tilde{d}_t$   
**for** each outer optimization update **do**  
**for** each  $c_{d,0} \in \bar{\mathcal{C}}$  **do**  
 Set  $a_0(c_{d,0}) \leftarrow \arg \max_{a \in \mathcal{A}} Q(s_0, 0, c_{d,0}, a; \theta)$   
**end for**  
 Set initial stock  $c_{d,0} \leftarrow \arg \max_{c \in \bar{\mathcal{C}}} \{-c + Q(s_0, 0, c, a_0(c); \theta)\}$   
**for** each environment step **do**  
 Observe state  $(s_t, t, c_{d,t})$   
 Select  $a_t \sim \epsilon\text{-greedy}(\arg \max_{a \in \mathcal{A}} Q(s_t, t, c_{d,t}, a; \theta))$   
 Execute  $a_t$ , observe  $r_{t+1}, s_{t+1}$   
 Compute the stock  $c_{d,t+1} \leftarrow (c_{d,t} + r_{t+1}) / \hat{d}_t$   
 Store  $(s_t, t, c_{d,t}, a_t, r_{t+1}, s_{t+1}, t+1, c_{d,t+1})$  in  $\mathcal{D}$   
**if** update is scheduled **then**  
 Sample batch  $\{(s^k, t^k, c_d^k, a^k, r^k, s'^k, t'^k, c_d'^k)\}_{k=1}^B$  from  $\mathcal{D}$   
**for** each sample  $k$  **do**  
 Compute  $a'^k \leftarrow \arg \max_{a \in \mathcal{A}} Q(s'^k, t'^k, c_d'^k, a; \theta)$   
**end for**  
**for** each sample  $k$  and horizon  $i$  **do**  
 Compute  $y_{i,j}^k \leftarrow r^k + \gamma_i \xi_{\bar{\theta}}(s'^k, t'^k, c_d'^k, a'^k)_{i,j}$  for  $j = 1, \dots, n$   
**end for**  
 Compute loss  $L_\theta$  using Eq. (20)  
 Update network:  $\theta \leftarrow \theta - \lambda_\theta \nabla_\theta L$   
 Update target network:  $\bar{\theta} \leftarrow (1 - \alpha) \bar{\theta} + \alpha \theta$   
**end if**  
**end for**  
**end for**


---

(from January 1998 to December 2017). The three index funds used are (i) Vanguard Total Bond Market II Index Fund Investor Shares (VTBIX), representative of U.S. Fixed Income; (ii) Vanguard Total International Stock Index Fund Investor Shares (VGTSX), representative of Foreign Equity; and (iii) Vanguard Total Stock Market Index Fund Investor Shares (VTSVX), representative of U.S. Equity. We model returns using a multivariate Gaussian distribution with mean vector and covariance matrix of respectively

$$\mu = \begin{bmatrix} 0.0493 \\ 0.0770 \\ 0.0886 \end{bmatrix} \quad \text{and} \quad \Sigma = \begin{bmatrix} 0.0017 & -0.0017 & -0.0021 \\ -0.0017 & 0.0396 & 0.0309 \\ -0.0021 & 0.0309 & 0.0392 \end{bmatrix}.$$

Table 2 displays the portfolio weights of each portfolio, ordered by risk aversion. One could also perform this analysis with true historical returns or simulations from alternative return distributions.

In Tables 3 and 4, we calculate Monte-Carlo estimations of some empirics using the optimal policy. The first column gives the undiscounted expected total utility, the second column indicates the probability of having sufficient wealth to attain the first goal, and the last two columns show the probabilities of achieving the different goals. Note that the return distributions of the portfolios were adjusted in each problem according to their horizon for comparison purposes, i.e.,  $\mu$  and  $\sigma$  when  $T = 10$  periods, and  $\mu/3$  and  $\sigma/\sqrt{3}$  when  $T = 30$  periods.

#### H.4 Atari 2600

The Atari 2600 benchmark, accessed via the Arcade Learning Environment [Bellemare et al., 2013], consists of a suite of classic video games with varied dynamics and reward structures. Our goal in this experiment is to illustrate the effect of the time-consistent formulation rather than to achieve state-of-the-art performance. Accordingly, and due to computational limitations, we run these experiments for 10 million steps and exclude particularly challenging games such as *Skating*, *Solaris*, *Montezuma's Revenge*, *Pitfall*, and *Private Eye* [Badia et al., 2020].

Table 2: Portfolio weights, where the most conservative (portfolio 1) has an expected return of 0.0526 and volatility of 0.0374, while the most aggressive (portfolio 15) has an expectation of 0.0886 and standard deviation of 0.1954.

PORTFOLIO WEIGHTS			
PORTFOLIO NUMBER	U.S. BONDS	INT'L STOCKS	U.S. STOCKS
1	0.9098	0.0225	0.0677
2	0.8500	0.0033	0.1467
3	0.7903	-0.0160	0.2257
4	0.7305	-0.0352	0.3047
5	0.6707	-0.0545	0.3837
6	0.6110	-0.0737	0.4628
7	0.5512	-0.0930	0.5418
8	0.4915	-0.1122	0.6208
9	0.4317	-0.1315	0.6998
10	0.3719	-0.1507	0.7788
11	0.3122	-0.1700	0.8578
12	0.2524	-0.1892	0.9368
13	0.1927	-0.2085	1.0158
14	0.1329	-0.2277	1.0948
15	0.0731	-0.2470	1.1738

Table 3: Evaluation of the learned optimal policies for a risk-neutral agent with  $c_{T/2}(1) = 100$  and  $c_T(1) = 150$  over 10,000 episodes, evaluated for 3 different runs.

METHOD	$\mathbb{E}[U]$	$\mathbb{P}[y_{T/2} \geq 100]$	$\mathbb{P}[\psi_{T/2} = 1]$	$\mathbb{P}[\psi_T = 1]$
$u_{T/2}(1) = 1000, u_T(1) = 1000, T = 10$				
$\mathbb{E}, \gamma = 1.00$	1104	0.848	0.848	0.256
$\mathbb{E}, \gamma = 0.99$	1112	0.845	0.845	0.267
$\mathbb{E}, k = 0.05$	1108	0.864	0.864	0.244
$u_{T/2}(1) = 1000, u_T(1) = 2000, T = 10$				
$\mathbb{E}, \gamma = 1.00$	1782	0.855	0.237	0.772
$\mathbb{E}, \gamma = 0.99$	1727	0.823	0.257	0.735
$\mathbb{E}, k = 0.05$	1757	0.844	0.283	0.737
$u_{T/2}(1) = 1000, u_T(1) = 1000, T = 30$				
$\mathbb{E}, \gamma = 1.00$	1082	0.770	0.770	0.312
$\mathbb{E}, \gamma = 0.99$	1093	0.802	0.802	0.291
$\mathbb{E}, k = 0.05$	1080	0.810	0.810	0.270
$u_{T/2}(1) = 1000, u_T(1) = 2000, T = 30$				
$\mathbb{E}, \gamma = 1.00$	1702	0.770	0.228	0.737
$\mathbb{E}, \gamma = 0.99$	1670	0.759	0.275	0.698
$\mathbb{E}, k = 0.05$	1612	0.735	0.438	0.587

In our experiments, we employ the standard Atari preprocessing pipeline, including frame skipping, grayscale conversion, resizing, frame stacking, and reward clipping. We adopt a convolutional architecture similar to Mnih et al. [2015] to encode visual observations. The input is a stack of four frames processed by three convolutional layers with 32 filters of size  $8 \times 8$  (stride 4), 64 filters of size  $4 \times 4$  (stride 2), and 64 filters of size  $3 \times 3$  (stride 1), each followed by ReLU activations. The resulting features are flattened into a 3136-dimensional vector. To augment the time step, a scalar time input is embedded via a fully connected layer with 64 units and ReLU activation and concatenated with the visual features. The combined representation is passed through a fully connected layer with 512 units and ReLU activation, followed by an output layer with  $n_{\text{act}} \times m \times n_{\text{quantiles}}$  units, representing quantile values for each action and discount factor.

We consider a multi-horizon risk-neutral agent, as described in Section 4, with a hyperbolic discount function as the time preference. The discretization of discount factors and the calculation of weights  $w(\gamma)$  are adopted directly from the open-source implementation provided by Fedus et al. [2019], available at [https://github.com/google-research/google-research/tree/master/hyperbolic\\_discount](https://github.com/google-research/google-research/tree/master/hyperbolic_discount). Their implementation

Table 4: Evaluation of the learned optimal policies for a risk-sensitive agent with  $c_{T/2}(1) = 100$  and  $c_T(1) = 150$  over 10,000 episodes, evaluated for 3 different runs.

METHOD	$\mathbb{E}[U]$	$\mathbb{P}[y_{T/2} \geq 100]$	$\mathbb{P}[\psi_{T/2} = 1]$	$\mathbb{P}[\psi_T = 1]$
$u_{T/2}(1) = 1000, u_T(1) = 1000, T = 10$				
CVaR <sub>0.1</sub> , $\gamma = 1.00$	999	0.998	0.998	0.001
CVaR <sub>0.1</sub> , $k = 0.05$	999	0.994	0.994	0.005
$u_{T/2}(1) = 1000, u_T(1) = 2000, T = 10$				
CVaR <sub>0.1</sub> , $\gamma = 1.00$	1007	0.986	0.986	0.010
CVaR <sub>0.1</sub> , $k = 0.05$	1020	0.977	0.977	0.022
$u_{T/2}(1) = 1000, u_T(1) = 1000, T = 30$				
CVaR <sub>0.1</sub> , $\gamma = 1.00$	920	0.848	0.848	0.073
CVaR <sub>0.1</sub> , $k = 0.05$	921	0.832	0.832	0.089
$u_{T/2}(1) = 1000, u_T(1) = 2000, T = 30$				
CVaR <sub>0.1</sub> , $\gamma = 1.00$	1014	0.895	0.889	0.062
CVaR <sub>0.1</sub> , $k = 0.05$	1015	0.842	0.842	0.087

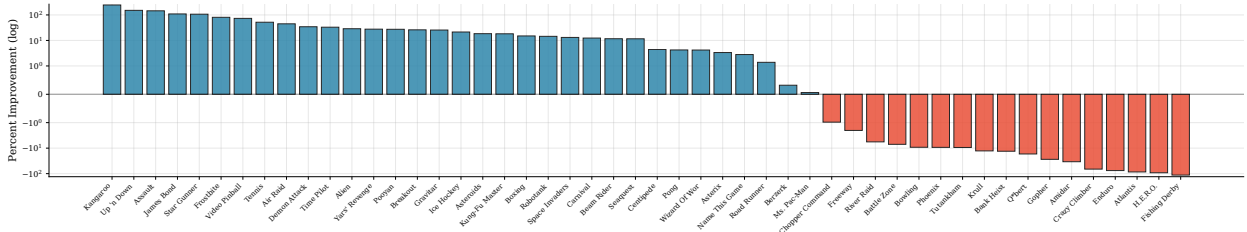


Figure 6: **Relative performance improvement of our Time-Consistent algorithm across 50 Atari games.** Each bar shows the percentage improvement in mean return for the Time-Consistent policy over the Time-aware Time-Inconsistent baseline, averaged over 3 seeds per game. The Time-Consistent policy outperforms the baseline in 33 out of 50 games. Across all games, it achieves a mean improvement of 15.73% and a median improvement of 8.02%, demonstrating the benefits of maintaining time-consistency under hyperbolic discounting.

consists of two steps: determining the set of evaluation discount factors and aggregating the resulting Q-values via a Riemann sum.

To ensure that the approximation covers the relevant range of time horizons up to a maximum effective discount  $\gamma_{\max}$ , the discount factors are selected using a power-law spacing. Specifically, for a hyperbolic coefficient  $k$  and  $m$  discount factors, the *evaluation gammas* (denoted  $\gamma_{\text{eval}}$ ) are generated as  $\gamma_{\text{eval}}^{(i)} = 1 - b^i$  for  $i = 0, \dots, m-1$ , where the base  $b$  is chosen to satisfy  $(1 - b^m)^k = \gamma_{\max}$ . This construction ensures that the largest  $\gamma$  used for Bellman updates corresponds to the target  $\gamma_{\max}$  after exponentiation.

The final hyperbolic Q-value is estimated as a weighted sum of the Q-values learned for each individual  $\gamma \in \Gamma$ . The weights correspond to the widths of the intervals in the Riemann sum. We use a lower Riemann sum approximation, where the weight  $w_i$  for the  $i$ -th Q-value is given by the difference between consecutive evaluation gammas:  $w_i = \gamma_{\text{eval}}^{(i+1)} - \gamma_{\text{eval}}^{(i)}$ . In our time-consistent formulation, these weights are updated dynamically as  $w_{i,t} = \frac{w_i \gamma_i^t}{\sum_{j=1}^m w_j \gamma_j^t}$ .

To ensure that differences in performance between our time-consistent agent and the time-inconsistent baseline are attributable solely to the evolving weight function and not simply to augmenting the state with the time step, we include a third approach in our analysis. In this method, which we call Time-Aware Time-Inconsistent, time is added to the state, but the agent continues to use the time-inconsistent weight functions.

In our experiments, we use  $m = 10$ ,  $\gamma_{\max} = 0.999$ , and  $k = 0.05$ . Figure 6 shows the performance improvement of our approach compared to the time-aware baseline; we observe that our approach outperforms this baseline in 33 out of 50 games, with an average improvement of 15.73%. Figure 7 shows the learning curves of the three approaches across 50 Atari games.

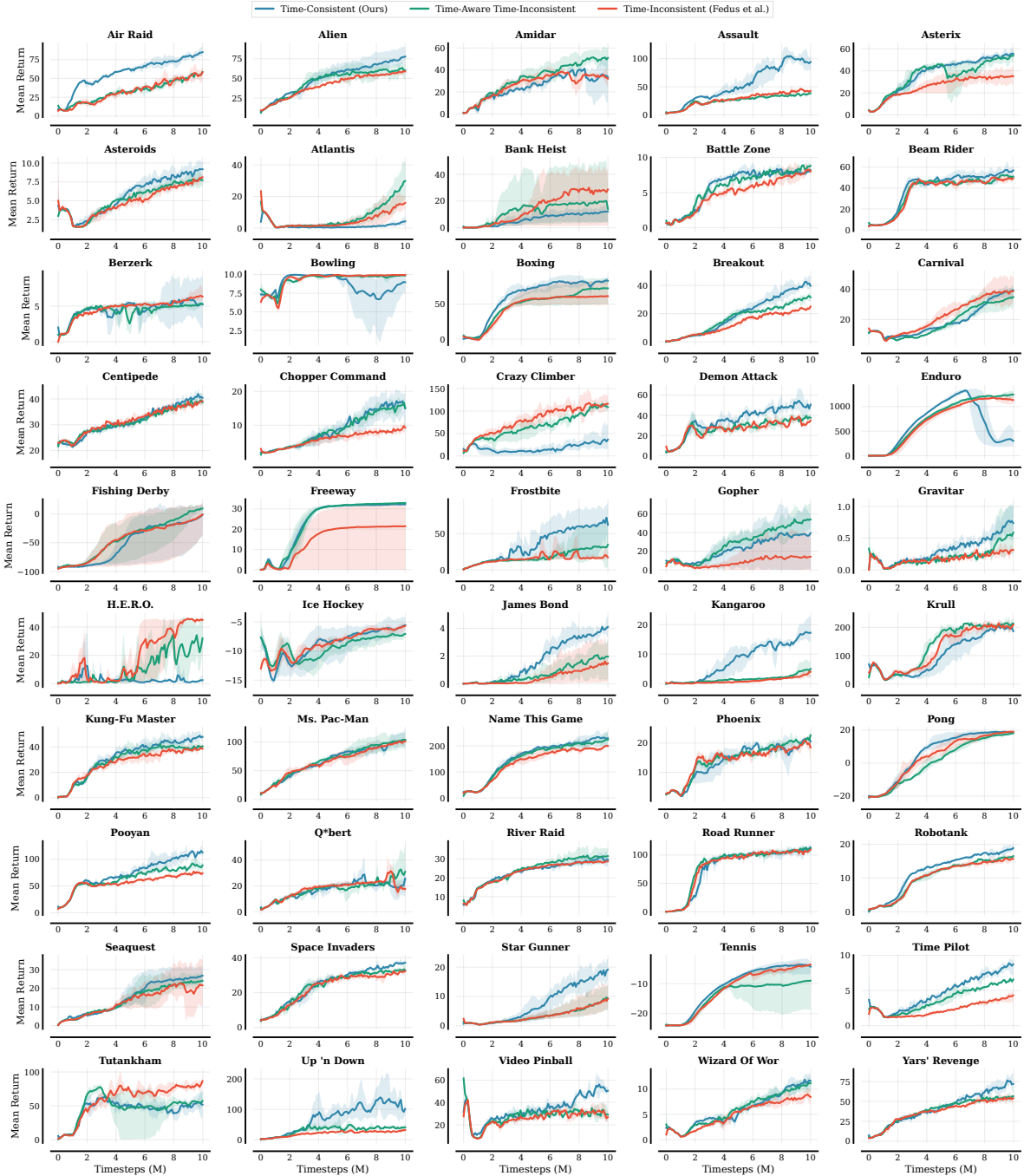


Figure 7: **Comparison on Atari 2600.** Learning curves over 10 million steps (40 million frames) for 50 Atari games. Our Time-Consistent agent (Blue) is compared against the Time-Inconsistent hyperbolic baseline from Fedus et al. [2019] (Red) and a time-aware variant of this baseline (Green). Shaded regions represent the standard deviation across 3 seeds. The results demonstrate that properly handling the non-stationarity of the optimal policy is critical for effective learning with general discount functions.